THE EFFECT OF MATERIAL AND PROCESS PARAMETERS ON IMPELLER TORQUE AND POWER CONSUMPTION IN A BLADED MIXER

by

PAVITHRA VALLIAPPAN

A thesis submitted to the

School of Graduate Studies

Rutgers, The State University of New Jersey

In partial fulfillment of the requirements

For the degree of

Master of Science

Graduate Program in Chemical and Biochemical Engineering

Written under the direction of

Benjamin J. Glasser

And approved by

_____

_____

_____

New Brunswick, New Jersey

October, 2018

ABSTRACT OF THE THESIS

The Effect of Material and Process Parameters on Impeller Torque and Power Consumption in a Bladed Mixer

By PAVITHRA VALLIAPPAN

Thesis Director:

Dr. Benjamin J. Glasser

A large number of industries including catalytic, chemical, cosmetic, food, and pharmaceutical industries frequently handle powders or granular materials in various unit operations. A cylindrical mixer mechanically agitated by an impeller blade is a common, industrially relevant geometry in numerous particle processing technologies. A bladed mixer has a capability of handling a wide variety of solid and liquid systems: free flowing and cohesive powders, pastes, or suspensions. The torque needed to move the impeller, provides insight into flow behavior of the material and can be monitored on the bench scale, pilot scale, and manufacturing scale so that it could provide useful information for scale-up and process monitoring & control. Experimental measurements of the agitation torque exerted on a particle bed and the power draw for the motor driving the impeller blades in a mixing process were conducted to investigate the impact of particle properties and blade geometry as a function of the blade rotation rate. It was found that the torque exerted on a granular bed and the power consumption were a strong function of the impeller blade configuration, the position of the blades in a deep granular bed, the fill height of the glass beads, and the size and friction coefficient of the particles. It was observed that the time-averaged torque and power

consumption for different particle sizes qualitatively scaled with particle diameter. A scale-up relationship for a deep granular bed was developed: the time-averaged torque and average adjusted power consumption scaled with the square of the material fill height.

ACKNOWLEDGEMENT

Firstly, I would like to express my sincere gratitude to my mentor and advisor Dr. Benjamin J Glasser for the continuous support of my Masters study, for his patience, motivation, and immense knowledge. His guidance helped me immensely throughout my research, professionally and personally. I could not have imagined having a better advisor and mentor for my Masters study.

I would also like to thank the rest of my thesis committee: Dr. Masanori Hara and Dr. Ravendra Singh, for their time, availability, insightful comments and suggestions.

With a special mention to Dr. Veerakiet Boonkanokwong without whose constant help and support I could not have completed this thesis. I also thank my fellow colleagues who were a part of Dr. Glasser's Particle Technology Research Group and in the Engineering Research Center for Structured Organic Particulate Systems (C-SOPS) at Rutgers University: Rohan Frank and Anusha Noorithaya for all the stimulating discussions, their friendship and support.

To all my friends at Rutgers University, and my extended family - the DOT group, thank you for being my family so far away from home.

Finally, I must express my very profound gratitude to my parents and my brother for providing me with love, unfailing support and continuous encouragement throughout my years of study and through the process of researching and writing this thesis. This accomplishment would not have been possible without them. Thank you.

TABLE OF CONTENTS

LIST OF FIGURES

the power draw at a specific RPM for the empty mixer from the power draw for the impeller in the mixer loaded with particles.

Fig. 7. Effect of the number of impeller blades on: (a) the average torque and (b) the average adjusted power as a function of the dimensionless shear rate. Impeller blades used in these sets of experiments have 135° angle and 45 mm length.

Fig. 8. Effect of the impeller blade angle on: (a) the average torque and (b) the average adjusted power as a function of the dimensionless shear rate. Impeller blades used in these sets of experiments have 4 blades and 45 mm length.

Fig. 9. Effect of the impeller blade length on: (a) the average torque and (b) the average adjusted power as a function of the dimensionless shear rate. Impeller blades used in these sets of experiments for both cases have 4 blades and 135° angle.

Fig. 10. Effect of the macroscopic friction coefficient (μ) of particles on: (a) the average torque and (b) the average adjusted power as a function of the dimensionless shear rate. Experiments were performed using the standard impeller blades and the glass beads with a diameter of 2 mm loaded to a 30-mm fill height (H/D = 0.30).

Fig. 11. Effect of the impeller blade position in a deep granular bed (90-mm fill height) on: (a) the time-averaged torque and (b) the average adjusted power as a function of the dimensionless shear rate, compared to those values in a shallow bed (30-mm fill height just covering the top tip of the blades). Blade position in a deep bed: top (H/D = 0.30), middle (H/D = 0.60), and bottom (H/D = 0.90). Experiments were performed using the standard impeller blades and the glass beads with a diameter of 2 mm.

Fig. 12. Effect of the particle size on: (a) the average torque and (b) the average adjusted power drawn from experiments as a function of the shear rate γ°. Experiments were

performed using the standard impeller blades, and the granular bed was filled up to a 30-mm height (H/D = 0.30) for all particle sizes.

Fig. 13. (a) The time-averaged normalized torque, $\langle T \rangle / d$, and (b) the average normalized adjusted power, P^*/d, plotted as a function of the shear rate $\dot{\gamma}$. Experiments were performed using the standard impeller blades, and the granular bed was filled up to a 30-mm height (H/D = 0.30) for all particle sizes. Note that the y-axis in Fig. 13b is multiplied by a factor of 10^3.

Fig. 14. Effect of the amount of materials in a bladed mixer, reported as the H/D ratio, on: (a) the time-averaged torque and (b) the average adjusted power as a function of the dimensionless shear rate. Experiments were performed using the standard impeller blades and the glass beads with a diameter of 5 mm. The effective H/D ratios indicate usage of a lead weight instead of using actual particle mass.

Fig. 15. (a) The time-averaged torque $\langle \vec{T} \rangle$ and (b) the average adjusted power P^* values in Fig. 14 were normalized by square of the height (H^2) of the granular material filled in a bladed mixer plotted as a function of the dimensionless shear rate. Experiments were performed using the standard impeller blades and the glass beads with a diameter of 5 mm. The effective H/D ratios indicate usage of a lead weight instead of using actual particle mass. Note that the y-axis in Fig. 15b is multiplied by a factor of 10^3.

1 INTRODUCTION

Mixing is a unit operation that is widely used in a variety of production processes ranging from catalytic to chemical, cosmetic, food, and pharmaceutical industries [1,2]. In pharmaceutical manufacturing, mixing is one of the steps of critical importance that needs to be carefully controlled. Homogeneity of a mixture of excipients and an active pharmaceutical ingredient (API) needs to be achieved to ensure that the drug concentration in a finished product is consistent and that all dosage units produced are of uniform potency [3]. There are several different types of mixers (also called blenders) used in the pharmaceutical industry. Examples of mixers include rotating drums [1], bladed mixers [3], high-shear mixers [4], agitated filter beds/dryers [5,6], and fluidized beds [7,8]. Bladed mixers and high-shear mixers have advantages that they are simple in construction and that they take a relatively short time to complete the mixing operation [9]. The degree of uniformity of dosage units and the resulting quality of finished products are functions of the material properties, the design of the mixer, and the operating conditions [10–12]. Process monitoring and control are therefore important to maintain stable product quality and improve process efficiency.

Monitoring of the mixing process can be carried out by various methods, such as employing the particle image velocimetry (PIV) technique [13], measuring agitation torque, and recording power consumption of the mixer [9]. While getting mixed, solid particulate matter exerts a load on agitator blades and vice versa, thus, giving rise to the

agitation torque [14]. Changes in powder characteristics and flow behaviors in the mixer are reflected by changes in the value of the impeller torque, e.g., when the endpoint of granulation is reached [9]. The torque required to turn an impeller in a particle bed depends on a number of factors, including blade design, agitator rotational speed, material fill level, and mixer size [15–17]. In the case where agglomeration is being carried out in a high shear mixer, torque measurement helps in control and monitoring of the granulation process [18–20]. Since torque is sensitive to changes in operating conditions, with rapid measurement and good precision, it can be used as a parameter to probe the efficiency of mixer designs [18]. In addition, impeller torque measured from a laboratory scale mixer can be used to characterize and predict the risk for agglomeration in powder beds with varying degrees of moisture content at industrially relevant scales. Bulk friction coefficient can also be measured for wet powder beds using torque data [21].

Impeller torque measurements can be implemented to monitor not only mixing and agglomeration/granulation processes, but also agitated drying processes. Drying of API crystals can be carried out in an agitated filter-bed dryer, which has advantages over tray dryers as it reduces operation time by improving heat and mass transfer. In an agitated dryer, torque data can provide a correlation between shear stress experienced by a powder bed and the degree of attrition of particles [5]. Impeller torque at the laboratory scale can also be used to obtain an estimate of the amount of work done per unit mass by the impeller at larger scales. This relationship can help improve scale up of the agitated drying process [5]. The ability to predict attrition and to obtain uniform size distribution

of API particles results in better critical quality attributes of the finished dosage forms including content uniformity, dissolution rate, bioavailability, and stability.

Besides the impeller torque measurement, recording power consumed by the impeller motor can also be employed to monitor and control mixing processes. Previous research by Ritala et al. [22] demonstrated that power consumption during rotation of the blades was a function of intra-granular porosity and surface tension of a binder solution in wet mixing operations. Additionally, a correlation existed between power consumption and the strength of the moist agglomerates. An increase in cohesiveness or tensile strength of the moist granule mass resulted in a change in power consumption, indicating that the liquid solution characteristics, such as surface tension and contact angle, had an influence on power consumption [22]. Jirout and Rieger [23] illustrated that, in the case of suspending solids in liquid systems, the power consumption required for off-bottom suspension of the solid particles could be used to compare the efficiency of different types/configurations of impellers for the mixing operation.

Although power consumption measurement has been extensively carried out in previous research on the liquid mixing process, there has been limited work for monitoring mixing of solids systems. With the current interest of moving from batch to continuous manufacturing in the pharmaceutical industry, continuous mixing processes have been extensively studied in recent years [24–26].

Vanarase et al. [27,28] conducted experiments on a continuous powder mixer to examine the effects of operating conditions, design parameters, and material flow properties of pharmaceutical mixtures as a function of shear rate. Relative standard deviation (RSD), one of the most common mixing indices, was used to characterize mixer's performance and in turn the efficiency of the mixing process. RSD is a measure of blend homogeneity, and for a continuous process they found RSD depended on several factors such as blade rotation rate, material flow rate, and mixer blade configuration. They demonstrated that the number of blade passes a measure of the strain, was a function of the blade rotational rate. Although there is interest in the pharmaceutical industry in continuous manufacturing, most products are still manufactured in batch mode. Thus, there is still a need to better understand batch operations.

Campbell [29,30] and Campbell and Brennen [31] outlined a theoretical method for calculating collisional stresses within a granular bed from the total contact force between particles, particle diameter, and volume of a sampling cell. The important stress tensor components in the area of granular material flows are the average normal stress and the shear stress. Knowing the normal stress values, the pressure inside a granular bed can be calculated. According to a granular rheological model [32,33] a number of experimental and numerical studies suggested that the mass density and the macroscopic (bulk) friction are functions of the inertial number, which can be computed from the shear rate, the particle diameter and density, and the compressive pressure. Stresses and torque can be measured from the macroscopic friction coefficient and the inertial number. In previous

work, Cavinato et al. [34] conducted experiments on the mixing and flow behaviors of cohesive pharmaceutical powders in lab-scale and pilot-scale high shear mixers. They proposed a scaling relationship based on a dimensionless torque number which was a function of the mass fill and the square root of the impeller Froude number. It was found that the mass fill was one of the important parameters that had an impact on the powder flow patterns during the high shear mixing process.

In spite of some previous research in this area, the roles of material properties, blade and equipment configurations, and operating parameters on the impeller torque and power consumption in a batch mixer are still poorly understood. In this thesis, we studied a bed of particles in a batch bladed mixer consisting of a cylindrical glass vessel and a vertical impeller blade. Particle properties and impeller blade configurations of the mixing system were varied to investigate their effects on the experimentally measured torque that the impeller exerted on particles and on the power consumption that the motor drew to move the blades through the granular bed.

2 MODEL AND EXPERIMENTAL SET UP

2.1 Experimental set-up and mixer geometry

The laboratory equipment used in this work is shown in Fig. 1. The unit was composed of a bladed mixer, a signal transducer with a load cell, a data recorder with a monitor, and a power meter. The unit is similar to what was used in previous work [5]. A cylindrical glass vessel and Teflon® impeller blades were purchased from Chemglass Life Sciences©. The glass chamber was affixed to a rotating table with a metal lever arm which applied force on a load cell when the blades moved through the particle bed. In the experiments, the impeller blades were attached to one end of a cylindrical stainless steel agitator shaft which was connected to a motor at the other end. The motor was firmly held on a Chemglass© bench top support stand and wired to a digital motor controller which was used to adjust the direction and the speed of rotation of the impeller blades. The data acquisition device used in this research was a Yokogawa™ DX1006-1. It was employed to record voltage signals to monitor the blade rotation speed and the force applied on the load cell (from which torque can be calculated). The power meter used in this study was a Vernier Software & Technology© Watts Up PRO; it was connected to the motor controller to measure power consumed by the impeller blades when rotated through a granular bed.

A schematic of the mixer geometry used in this work is depicted in Fig. 2, and the dimensions of the bladed mixer are reported in Table 1. The cylindrical vessel has an inner

diameter (D_0) of 100 mm and a total internal height of 155 mm, which can hold a volume of approximately 1.2 liters. The mixer is mechanically agitated by impeller blades, and the agitator shaft is placed at the center of the cylindrical mixer. The diameter of the cylindrical impeller shaft (D_1) is 10 mm, and H_0 is the height above the blades which is 128 mm for our standard setup. The vertical span of the impeller blades (H_1) is 25 mm, and the length (L) of each blade measured from the center of the impeller shaft to the edge of the blade is mm for the initial impeller blades used in this work. The clearance between the bottom of the blades and the base of the mixer (H_2) is set to approximately 2 mm in all experiments.

2.2 Materials

The granular material used in this research was Dragonite® composite glass beads (Jaygo Incorporated, Randolph, NJ) with a density of 2500–2550 kg/m3. Physical properties of the cohesion-less spherical glass beads used in the experiments are listed in Table 2. Three different diameter sizes of the beads were utilized in the experiments: 1 mm (0.60–1.40 mm), 2 mm (1.70–2.36 mm), and 5 mm (4.71–5.01 mm). Particle size distribution analysis of the glass beads was conducted using sieve analysis, and the ranges for the three different particle diameters were reported in the parentheses above. The glass beads of the 1-mm diameter were colorless, and the 5-mm particles were surface-colored purple. Two types of 2-mm glass beads were used in the experiments: surface-colored red beads and clear beads. The 2-mm red glass beads were used for our initial experiments while

the 2-mm colorless glass beads were used for subsequent particle surface roughness modification experiments which will be described later in Section 2.4. It was noticed that after running the experiment for some time, particles started to stick to the walls of the vessel. An anti-static ionization blower and anti-static spray were therefore used to reduce static charges [35] and to produce reliable and repeatable results.

2.3 Impeller torque and power measurement protocol

Before performing each experiment, the impeller shaft was first placed at the center of the bladed mixer, and then glass beads were gently loaded into the mixer and allowed to settle while the blades remained stationary. Blade movement was then started, and the signal measurement and recording were commenced. The impeller blades were rotated in the counter-clockwise direction leading to an obtuse-angle blade orientation which is a commonly used configuration in industry. Experiments were carried out at various blade rotational speeds ranging from 10 to 200 revolutions per minute (RPM). At these shear rates, granular flows in the bladed mixer occurred in the quasi-static and intermediate regimes according to the flow regime map proposed by Tardos et al. [36]. When starting the blade movement, the rotational speed of the impeller was gradually increased from 0 RPM to a desired rotation rate for each experiment. In this research, the signal data was measured and recorded once every second for the time-averaged torque and every 0.125 seconds for the torque fluctuation analysis. The total time duration for recording signals for each individual experiment was 3 minutes and 30 seconds, and for each blade

rotational speed the experiment was repeated three times. Mean and standard deviation of instantaneous data at each time step were calculated from the three separate data sets. In general, the steady state of a system was usually reached within 30 – seconds of the blade movement for all experiments. Once the steady state was reached, the time averaging procedure for the mean torque and power readings was achieved throughout the measurement period.

The torque was measured by measuring a force and multiplying this by the lever arm length. In this set-up, force was measured by using a load cell attached to a metal arm that pivots around a rotating table in which the glass vessel assembly sits, as shown in Fig. 1. As the impeller moves through the granular bed, the blades transmit force to the particle bed causing the material to rotate relative to the mixer wall. The rotation of the glass vessel causes the pivot arm to apply force on the load cell which measures the force. With this set-up, torque can be calculated from cross-multiplying the length of the lever arm and the measured force:

$$\vec{T} = \ell \times \vec{F} \qquad (1)$$

where $\vec{T}$ is the torque acting on the load cell, ℓ is the lever arm length, and $\vec{F}$ is the measured force that the lever arm acts on the load cell.

It can be shown that the torque exerted on the impeller at the shaft equals the torque exerted on the mixer (walls) due to the moving granular bed [37]. Knowing the agitation torque, the average shear stress experienced by the granular bed can be computed from the equation given by Darelius et al. [5,38]:

$$\langle \tau_{\theta r} \rangle = \frac{\vec{T}}{2\pi R_{\mathrm{cyl}}^2 H_{\mathrm{m}}} \qquad (2)$$

where $\langle \tau_{\theta r} \rangle$ is the average shear stress, $\vec{T}$ is the measured impeller torque, R_{cyl} is the radius of the cylindrical glass mixer, H_{m} is the height of the moving particle bed when the blades are rotating. Moreover, work done by the impeller can be calculated from the impeller torque by using the following expression:

$$W = \int_0^t \vec{T} \cdot \omega dt \qquad (3)$$

where W is the work done by the impeller blades over time t, $\vec{T}$ is the impeller torque, and ω is the angular velocity of the impeller blades.

As described above, the torque measured in our experiments is the torque needed to move the granular bed. However, for power consumption measurement, the power is made up of two components. One component is the power needed to run the motor, and the other is the power needed to move the particle bed. The power needed to run the

motor is therefore subtracted from the actual power reading measured by the power meter when a mixer is loaded with particles:

$$P^* = P - P_{emp} \quad (4)$$

where P^* is an adjusted power for the charged cylinder for a given RPM, P is the actual power measured by the power meter for the charged cylinder for a given RPM, and P_{emp} is the power measured for an empty mixer at that same RPM. All powers are measured in watt (W).

2.4 Particle surface roughness

A method for modifying the surface of glass beads is described by Remy et al. [39], and this protocol was adopted in this study in order to investigate the effect of particle surface friction on the impeller torque and power. In this procedure, a rotating drum was employed to coat the surface of 2-mm colorless glass beads with magnesium stearate (MgSt). Magnesium stearate was chosen as a coating material due to the increased asperity and the irregular shape of its primary particles. The adhesive interaction between MgSt and the surface of the glass beads occurred to physically coat the glass beads with MgSt. The magnesium stearate was purchased from Sigma-Aldrich® (CAS No. 557-04-0) and was composed of irregular plates with a mean diameter of 15 µm. The rotating drum used as a coater was made out of glass with an outer diameter of 20.5 cm and a length of

8 cm. The rotating drum contained 4 Teflon® baffles equally spaced along the side wall of the drum. The baffles were 3 cm deep and 7 cm in height. The protocol for particle surface roughening is briefly mentioned as follows. In total 200 – 400 g of the beads were added into the rotating drum, followed by 50 – 100 g of MgSt to achieve a 25% w/w MgSt concentration. The drum was rotated at 30 RPM under atmospheric pressure for 15 minutes. Some small MgSt agglomerates were created during the coating procedure. The resulting mixture was sifted through No. 8 and No. 12 sieves in order to separate the coated beads from the MgSt agglomerates. The resulting MgSt-coated glass beads had a particle diameter ranging from 1.7 mm to 2.4 mm, a size range similar to that of the uncoated glass beads (see Section 2.2). Using a Freeman Technologies FT4 rheometer, a macroscopic/bulk friction coefficient (μ) was measured. For the 2-mm MgSt-coated glass beads the macroscopic friction is 0.38 ± 0.008 compared to 0.32 ± 0.009 for the uncoated beads [39]. MgSt is universally known to be a lubricant for pharmaceutical powders when it is added to pharmaceutical powders in small quantities (up to around 1.5% w/w). At the same time, it has been observed that when added in large quantities (around 25% w/w) to glass beads, it serves to increase the macroscopic friction coefficient of the glass beads [39]. This is because at a particle surface level MgSt-coated beads have some surface roughness and irregularity due to the increased asperity and the irregular shape of the MgSt primary particles while the uncoated glass beads have a fairly smooth surface. Results for the effect of particle surface roughness on measured impeller torque and power consumption will be discussed in Section 3.3.

2.5 Figures for Chapter 2

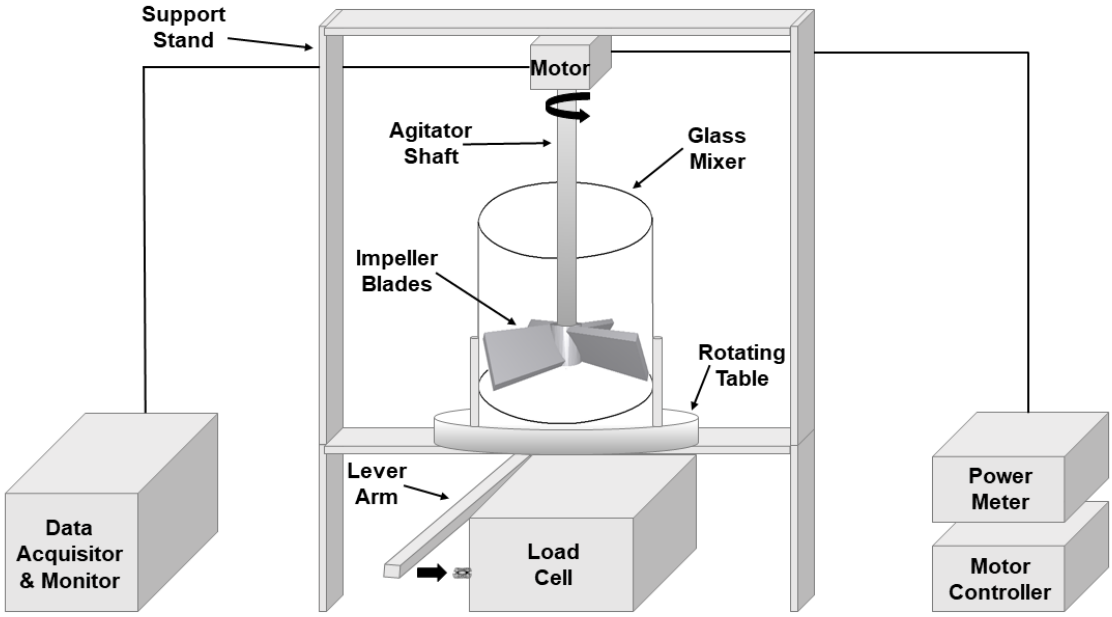

Fig. 1. A schematic of the laboratory experimental set-up for the impeller torque and power measurements.

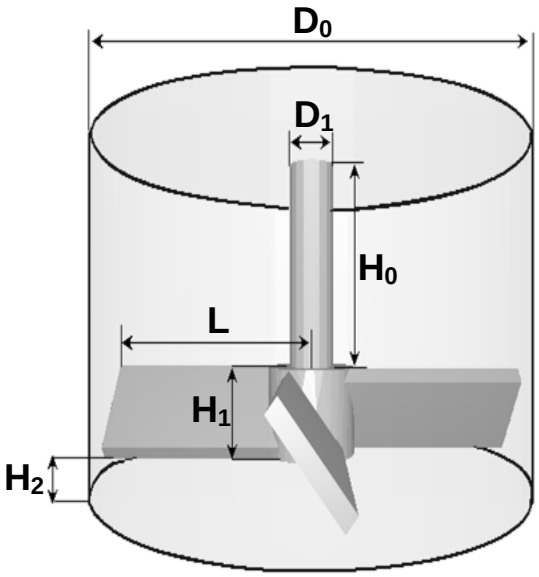

Fig. 2. A schematic of the 4-bladed mixer used in the experiments.

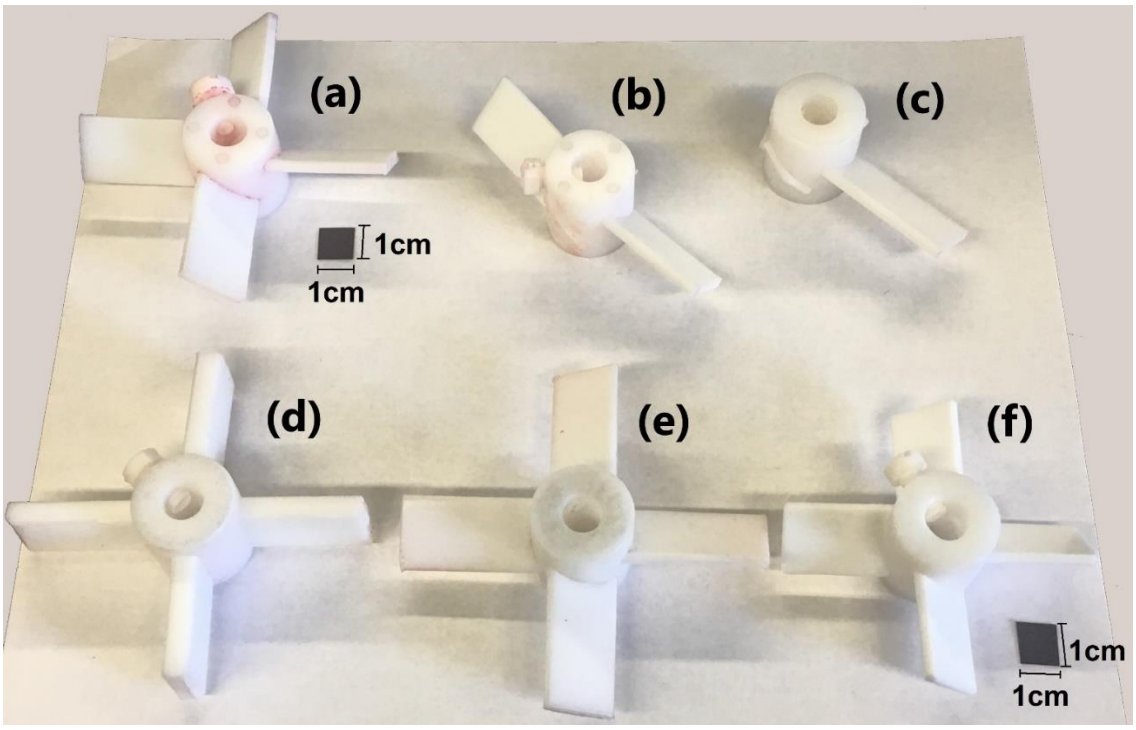

Fig. 3. Impeller blade configurations used in the experiments: (a) standard impeller, 4 blades, -mm length, 135° angle; (b) 2 blades, 45 mm length, 135° angle; (c) 1 blade, 45 mm length, 135° angle; (d) 4 blades, 45 mm length, 90° angle; (e) 4 blades, 45 mm length, 150° angle; and (f) 4 blades, 37.5-mm length, 135° angle. The black squares in this figure show an area of 1×1 cm^2.

2.6 Tables for Chapter 2

Variable	Symbol
D_0	100
D_1	10
L	
H_0	128
H_1	25
H_2	2

Table 1: Laboratory mixer dimensions.

Variable	Symbol	Value
Particle diameter	*d*	1, 2, and 5 mm
Particle density	ρ_p	2.50–2.55 g/ml
Macroscopic friction coefficient (uncoated beads)	μ	0.32
Mass of granular bed	*m*	300–900 g

Table 2: Glass bead properties used in experiments.

3 RESULTS AND DISCUSSION

3.1 Granular Flow in a Shallow Bed

In this section, we first consider granular flows in a shallow bed, which we will refer to as "the base case". In our base case the 2-mm monodisperse, cohesion-less, spherical, uncoated red glass beads were used. The amount of a granular material loaded in the mixer was approximately 300 g, which was sufficient to cover just the top tip of the impeller blades, and the initial fill height of the stationary particle bed, H, was measured as 30 mm (H/D = 0.30). Experiments were performed in the bladed mixer with dimensions given in Table 2. The impeller (Fig. 2) used in experiments in this part consisted of 4 blades pitched at 135° angle with respect to a horizontal plane, and each blade had a length of mm, which we will consider as "the standard impeller blades".

3.1.1 Torque and Power Measurements

The protocol described in Section 2.3 was followed, and the torque signals were measured and recorded every second for experiments in this section. The time-averaged torque and the average adjusted power are plotted as a function of the dimensionless shear rate (γ*) as shown in Fig. 4.1. The dimensionless shear rate (γ*) is defined by the following equation according to Tardos et al. [36]:

$$\gamma* = \gamma^{\circ}\sqrt{\frac{d}{g}} \qquad (5)$$

where γ° is the shear rate (s^{-1}), d is the diameter of particles (m), and g is the gravitational acceleration (m/s^2). The shear rate (γ°) can be computed from the blade rotational speed (in RPM) by using the formula:

$$\gamma^{\circ} = 2\pi \times \frac{\text{Rotational Speed}}{60} \qquad (6)$$

In Fig. 4a, it can be seen that the average torque increases linearly with the blade rotational speed. One may expect that there would be two granular flow regimes as described by Tardos et al. [36]. The first one is the quasi-static or slow regime (γ* is smaller than ~ 0.1). The second regime is called the intermediate regime (γ* >~ 0.1). In the quasi-static regime one would expect the torque to be independent of rotation rate. We do not observe such a regime for a shallow particle bed (H/D = 0.30). We will come back to this point when we examine deep beds as in that case we do observe a quasi-static regime where torque is independent of shear rate. The trend of the linear increase in torque as a function of shear rate in the intermediate regime observed from experimental results in this section are qualitatively similar to numerical results from previous research studies using a discrete element method (DEM) computational technique done by Chandratilleke et al. [15] and Sato et al. [9].

Fig. 4b displays a graph of the average adjusted power plotted as a function of the dimensionless shear rate. The adjusted power (P*) was obtained by subtracting the power

consumed at a specific RPM with an empty cylinder from the power consumed by the impeller in the mixer loaded with particles. Similar to the torque graph in Fig. 4a, the average adjusted power linearly increases for the entire range of the dimensionless shear rate. In this research, it is assumed that the power needed to run the motor under load can easily be separated from the power needed to move the impeller by subtracting the power needed to run the motor when the mixer is not under load (i.e., when the mixer is empty and has no particles charged). However, this assumption might not be always true for all settings. Nevertheless, the power consumption measurement still provides useful information for pharmaceutical and other industries dealing with mixing processes, but care needs to be taken since recording power data is not as easily interpreted as measuring torque.

3.1.2 Fluctuation Analysis of Torque Data

The torque signals were measured and recorded every 0.125 seconds for all the experiments in this part. The instantaneous torque values $\langle\vec{T}\rangle$ measured at each time step were normalized by the time-averaged torque, $\langle\vec{T}\rangle$ at each blade rotational speed:

$$\vec{T}^{*} = \frac{\vec{T}}{\langle\vec{T}\rangle} \qquad (7)$$

where $\vec{T}^{*}$ is the dimensionless normalized torque at each time step. Fig. 5a – d display the normalized torque $\vec{T}^{*}$ fluctuation profiles after the particulate systems have reached a

steady state for different blade rotational speeds: 10 RPM, 20 RPM, 60 RPM, and 200 RPM, respectively. The time span shown in these graphs is 25 seconds and was sampled from the middle period of the experiments at steady state. The smallest fluctuation amplitudes can be seen in the case where the impeller blades rotate at 10 RPM (Fig. 5a). The torque fluctuation profiles for 10 RPM (Fig. 5a) are comparable in amplitude to those for 20 RPM and 60 RPM (Fig. 5b – c, respectively). As the shear rate increases in the intermediate regime of granular flow, i.e., increasing the blade rotational rate from 60 RPM (Fig. 5c) to 200 RPM (Fig. 5d), the fluctuation amplitudes increase. At 200 RPM (Fig. 5d), there is a noticeable recurrence of a periodic burst behavior of the torque fluctuations, indicating low and high values of torque which we conjecture are due to the expansion and compression states of the granular bed in the highest shear rate case of our experiments.

3.1.3 Fast Fourier Transform (FFT) of Torque Data

We also computed the discrete Fourier transform of the torque signals using the fast Fourier transform (FFT) algorithm in MATLAB® for the same blade rotation rates mentioned in Section 3.1.2. Torque data input for the FFT was measured and recorded every 0.125 seconds. Single-sided amplitude spectrums of the FFT torque data are depicted in Fig. 6 for various rotational speeds of the impeller blades corresponding to Fig. 5. As a check of the algorithm, we confirmed that the values of the 0-Hz components (the peaks at 0 Hz) always corresponded to the time-averaged torques for each blade

rotation speed. Peaks corresponding to the impeller blade rotational rates (in RPM) can be observed (as circled for each rotational speed in Fig. 6), and the frequency (f) of each peak in Hz can be calculated by the following formula where the rotational speed is in RPM:

$$f = \frac{Rotational\ Speed}{60} \tag{8}$$

For example, the peak at frequency of 0.167 Hz can be seen in Fig. 6a for the impeller blades rotating with 10 RPM. The height of the blade frequency peaks increases with an increase in the rotational speed of the impeller blades. It is interesting to note that there are several overlapping peaks occurring between 2 – 3 Hz for all shear rates. We hypothesize that these peaks between 2 – 3 Hz are associated with natural frequencies of the moving granular material itself. It is also important to state that in all cases these peaks are higher in amplitude than the rotating blade frequency peaks.

3.2 Effect of Impeller Blade Configurations

A photo of the different types of the impeller blades used in our experiments is presented in Fig. 3. The black squares in this figure show an area of 1 × 1 cm^2. Fig. 3a is what we referred to as “the standard impeller blades”. In this part we explore the effects of the impeller configurations on the measured torque and power by changing the number, the angle, and the length of the blades using the impellers in Figs. 3b – f.

3.2.1 Effect of the Number of Impeller Blades

DEM simulations have been used by Boonkanokwong et al. [40] to study the effect of the number of impeller blades on granular flow behaviors and mixing kinetics in an agitated mixer. Different numbers of the blades in a mixer resulted in different impeller contact forces and particle velocity profiles, and thus, different mixing performance. The number of the blades used in a mixing system can also affect the impeller torque exerted on granular materials in a mixer and the equipment power consumption. This will be experimentally investigated further in this section. Experiments were carried out with different sets of impeller blades used in a mixer: 4 blades, 2 blades, and 1 blade as shown in Figs. 3a – c, respectively. All of these impeller blades are pitched at a 135° angle and have the same length (L) of 45 mm. The 2 and 4 blades are symmetrically placed about the vertical axis of the impeller shaft. All other particle parameters and operating conditions were the same as in the base case discussed in Section 3.1.

In Fig. 7a, the time-averaged torque for different blade numbers is plotted as a function of the dimensionless shear rate. The trends of how torque behaves as a function of the impeller blade rotational rate for the 1- and 2-bladed mixers are similar to that for the 4-bladed mixer (see Section 3.1.1). Interestingly, the average torque measured in the 2-bladed mixer is larger than that in the 4-bladed mixing system at all blade rotational speeds, and the value measured from the single-bladed mixer is significantly less than that of the 2 and 4 blades cases. In previous work [40], it was found that higher radial and vertical velocities of particles were observed in the 1- and 2-bladed mixers, which led to

more pronounced three-dimensional recirculation patterns. However, the tangential velocity components of particles in the 3- and 4- bladed cases were larger. Additionally, it was found that using two or three impeller blades provided better mixing performance than using one or four blades, as evaluated by calculation of the relative standard deviation (RSD) and the Lacey index of the systems. Granular temperature and particle diffusivities obtained for the 2- and 3-bladed cases were also higher than those for the 1- and 4-bladed mixers. Solids fraction analysis showed that dilation of the particle bed occurred to the greatest extent in the 2-bladed mixer. In our work we observe that the average torque measured in the 2-bladed mixer is larger than that in the 4-bladed mixer at all blade rotational speeds, and the value measured from the 1-bladed mixer is significantly less than those of the 2 and 4 blades cases. We hypothesize this is due to the fact that in the 1-bladed mixer the averaged tangential contact force that the impeller blades exert on particles is less than that in the 4-bladed mixer which is in turn less than that in the 2-bladed mixer [40]. The average adjusted power is presented in Fig. 7b, and it can be seen that the 1-bladed mixer has lower values than that of the 2- and 4-bladed mixers. In addition, the average adjusted power for the 2-bladed case is higher than the 4-bladed case which is in agreement with the torque measurements (see Fig. 7a). The trend of a linear increase of the adjusted power with an increase in the shear rate is observed for all numbers of blades used in this section. The fluctuations of both torque and power values at each rotation rate in the 1-bladed mixer are generally higher than those in the 2- and 4-bladed cases because of asymmetry of the single blade when rotating through a granular bed.

We should note that both the torque and power that we measure go to zero when the rotational speed is zero. At the same time, for both Fig. 7a and b, if you extrapolate the data back to a zero rotational speed, it looks like there will be a finite value of torque and power at zero rotational speed. This is because we are not able to collect data at very low dimensionless shear rates; we cannot go below a dimensionless shear rate of around 0.01 in Fig. 7. This is due to the fact that we cannot get our motor to move the impeller through the granular bed at very low rotation rates. Our motor does not have enough power/torque at low rotation rates to start moving, and it therefore becomes stuck in the granular bed. Further work would be needed with a more sophisticated motor that can operate at very low rotation rates, to discern the exact behavior at low rotation rates. Moreover, we expect complex behavior at very low rotation rates including stick-slip phenomena.

3.2.2 Effect of the Impeller Blade Angle

We next explore the effect of varying the impeller blade angle on granular flow properties. For the standard impeller (Fig. 3a), blades are pitched at a 135° angle with respect to the horizontal plane. The angles of the blades used for the experiments in this section were altered to 90° (Fig. 3d) and 150° (Fig. 3e). The impellers were set to rotate in the counter-clockwise direction to provide obtuse blade angle configurations, which are commonly used in industries and considered to result in better mixing performance than the acute angles [41]. All other particle parameters and operating conditions were

the same as in the base case. Time-averaged torque and average adjusted power plotted as a function of the dimensionless shear rate are displayed in Fig. 8. From Fig. 8a, it can be seen that the blades with 90° angle have the highest average torque values, followed by 135° and 150° angles, respectively. In general, the torque values for the 135° and 150° cases are quite similar.

In Fig. 8b, it is seen that the average adjusted power readings for the three different blade angle configurations are closer to one another than the torque values (see Fig. 8a). We observe in general less differences in power than in torque. We hypothesize that this is because measuring power consumption is more complicated than measuring the torque since power is composed of two components (the power needed to run the motor and the power needed to move the granular bed). We wanted to report values for the power required to move the particle bed (i.e., the adjusted power). We therefore measured the total power drawn by the motor and computed the adjusted power by subtracting out the power needed to run the motor when the mixer is empty from the total power meter readings (at the same impeller blade rotational speed). We make the assumption that the power needed to run the motor when the mixer is charged with particles is equal to that when the mixer is empty, which might not be true for all settings and may partly contribute to the fact that there is no significant effect of different blade angles on the adjusted power at low impeller rotational speeds. In general, the average torque and the adjusted power decrease with an increase in the impeller blade angle. Our experimental data is in good agreement with the DEM simulation results accomplished by

Chandratilleke et al. [15], examining the effect of rake angle of the impeller on the shaft torque for cohesive particles in a vertical bladed mixer.

3.2.3 Effect of the Impeller Blade Length

We next investigate the effect of the length (L) of blades by using two different types of impeller configurations in our experiments: the -mm standard blades (Fig. 3a) and the 37.5-mm blades (Fig. 3f). Both impellers have four blades with a 135° angle. All other particle parameters and operating conditions were the same as in the base case. In Fig. 9a, it is noticed that when the time-averaged torque is plotted as a function of the dimensionless shear rate, torque values for both blade lengths increase fairly linearly with shear rate. In addition, the time-averaged torque of the 45 mm blades is significantly higher than that of the 37.5-mm blades for the entire range of impeller rotational rates.

It can be observed in Fig. 9b that the average adjusted powers at low shear rates are not obviously different for the two blade lengths. We hypothesize that this is for similar reasons to what was discussed earlier for Fig. 8b, i.e. measuring the power consumption is complex in nature. We have assumed that the power needed to run the motor when the mixer is not under load (empty mixer) equals the power needed to run the motor when the motor is under load (charged mixer). As we discussed previously, this assumption may not be true for all conditions and may contribute to the adjusted power results being similar especially for low rotational speeds of the impeller blades. However,

at higher shear rates as the dimensionless shear rate increases, the average adjusted power is higher for the 45 mm standard blades than the 37.5-mm blades.

3.3 Effect of Particle Friction Coefficient

Remy et al. [39] experimentally and computationally studied the effect of varying roughness of particle surface on granular flow behaviors and mixing kinetics. They found that particle friction had a tremendous impact on particle velocity profiles and mixing patterns of granular materials in a bladed mixer. In this section, the effect of particle surface roughness on impeller torque and power will be investigated. The experiments were conducted for two sets of 2-mm glass beads; one was the standard uncoated red beads, and the other was the magnesium stearate (MgSt)-coated colorless beads fabricated according to a protocol in Section 2.4.

The fill height of the particle bed for both cases was 30 mm (H/D = 0.30). The standard impeller blades (Fig. 3a) were used, and all other operating conditions were as in the base case. The results for the effect of roughness of the particles on the measured torque and adjusted power are shown in Fig. 10. It is observed in Fig. 10a that the MgSt-coated beads (m = 0.38, see Section 2.4) exhibit a distinctively higher average torque than the uncoated beads (m = 0.32, see Section 2.4). The reason for this is that the coated beads have a higher friction than the uncoated beads, and thus the impeller blades require more force to move through the particle bed. Also, the standard deviations of the torque values at

each rotational rate are more for the MgSt-coated beads than those in the regular bead case as shown by the magnitude of the error bars in Fig. 10a. As shown in Fig. 10b, the average adjusted power for the uncoated beads is noticeably less than that of the MgSt-coated beads for the entire range of the impeller blade rotational speed. These trends of torque and power consumption as a function of shear rate are similar to results for an experimental study performed by Remy [42] and DEM simulations carried out by Benque [43].

3.4 Effect of Impeller Blade Position in a Deep Granular Bed

Remy et al. [41] demonstrated via DEM computational studies that granular flows in a shallow bed behaved differently from those in a deep particle bed. In this part, we will experimentally compare the measured agitation torque and the power consumption for shallow and deep beds. The granular material used in this section's experiments was 2-mm red colored glass beads, and the amount of material loaded into the laboratory mixer was increased from an initial bed height of 30 mm (as in the base case) to 90 mm.

It should be noted that we observed in our experiments that when the blades are rotating the total height of the granular bed is approximately the same as the granular bed initial height at a stationary state. The particle bed with a 30-mm fill height (H/D = 0.30), i.e., the amount of glass beads just covering the top tip of the blades, was considered to be the shallow bed, and the particle bed with a 90-mm fill height was considered to be the deep bed.

The H/D ratios in the deep bed are calculated from the height of the glass beads that cover and are above the span of the impeller blades, i.e., H is defined as the height from the bottom of the blades to the top of the granular bed. This was done as it had been shown previously that the material above the blades affected torque measurements [41,]. In order to investigate this impact, the blade position in a deep granular bed was changed from the bottom (H/D = 0.90) to the middle (where the blades are at 30-mm height from bottom, H/D = 0.60) and to the top (where the blades are at 60-mm height from bottom, H/D = 0.30) in the mixer, compared to results in the shallow bed (30-mm fill height, H/D = 0.30). The standard impeller blades (Fig. 3a) were used, and all other process parameters in the experimental set-up were the same as those in the base case. Comparison between the shallow and the deep granular beds for the measured torque and power plotted as a function of a dimensionless shear rate is shown in Fig. 11.

From Fig. 11a, one can see that the time-averaged torque for the deep bed cases for H/D = 0.60 and 0.90 are considerably larger than that for H/D = 0.30. In addition, the deep and shallow bed cases for H/D = 0.30 agree fairly well. For the deep bed cases of H/D = 0.60 and 0.90, we now see that for low shear rates there is a quasi-static region (for γ^* less than approximately 0.05) where the torque does not vary with shear rate. For the intermediate regime (γ^* larger than approximately 0.05), the torque values linearly increase as the blade rotational speed increases for all cases in the deep bed. Depicted in Fig. 11b, the average adjusted power for the deep bed increases with a relatively large slope as the impeller rotation rate increases; whereas, the power for the shallow bed

increases with a relatively smaller slope as the blade rotational speed increases. From Fig. 11a and b, it can be seen that the time-averaged torque as well as the average adjusted power for the blades at the bottom case (H/D = 0.90) are significantly larger than those for the cases in which the blades are at the middle position (H/D = 0.60) and at the top position (H/D = 0.30) in the deep granular bed, respectively. This is because as the amount of materials on top of the blades increases, the hydrostatic pressure applied on the impeller increases, and thus, the resulting shear stress also increases correspondingly (see Eq. (10)).

It can be observed that the average torque and the adjusted power results for the blades at the top position (H/D = 0.30) in the deep bed case are not significantly different from those for the shallow bed case (30-mm fill height in which particles are just covering the top tip of the blades with the impeller at the bottom of a mixer, H/D = 0.30). As was discussed, it has been shown in previous work [41,] that the materials underneath the impeller blades do not have any substantial influence on flow of grains in a mixing system since the only portion of a granular bed that moves is material within the span of the blades or close to the blades. The H/D = 0.30 case for the shallow and deep beds (see Fig. 11) are not identical; the small differences may be due to the fact that while the impeller at the top of a deep bed is rotating, the blades push some portion of the glass beads downward and cause some particles below to move which affects the agitation torque and power values.

3.5 Effect of Particle Size and Scaling Relationship

Particle size is one of the important material properties that plays a crucial role in granular flow and mixing. To understand the effect of particle size on power and torque exerted by an impeller blade on a granular material, three different particle sizes were examined in our experiments: 1-mm, 2-mm, and 5-mm diameter glass beads. All experiments in this section were performed using the standard impeller blades (Fig. 3a), and the fill height of the particle bed was kept constant to be 30 mm (H/D = 0.30) for all particle size cases. In addition, all other parameters and processing conditions were set to those in the base case.

In previous sections, the average torque and power values were plotted as a function of the dimensionless shear rate (γ^*). However, when plotting in this manner, the data points for different bead sizes do not lie on the same x-axis scale, making it more difficult to interpret the results. This is because the dimensionless shear rate (γ^*) is a function of particle size itself (see Eq. (5)).

Therefore, in order to fit data points on the same x-axis scale, for this section only the time-averaged torque, as well as the average adjusted power, are plotted as a function of the shear rate ($\gamma°$), as shown in Fig. 12. In Fig. 12a, the average torque measured for the 5-mm diameter particles is the highest, followed by the values for 2- mm and 1-mm beads, respectively. A trend of linearly increasing torque values as the blade rotational rate increases can be observed for the 1-mm particles, similar to the 2-mm case (the base case

in Fig. 4). At low shear rates ($\gamma^\circ < 4\ s^{-1}$) fairly constant torques are observed for the 5-mm beads indicating a quasi-static regime, and for higher shear rates there are linearly increasing torque values (indicating an intermediate regime) as the shear rate (or the blade rotational rate) increases. Similar trends are generally observed for the adjusted power graph in Fig. 12b, but the values linearly increase with shear rate for all particle sizes. Jop et al. and Andreotti et al. [46] have observed that granular flows can be characterized by a dimensionless inertial number which is proportional to the particle diameter, d, so it is possible that we may be able to scale the agitation torque by the particle diameter and have the results collapse on top of another. In addition, the power consumption of the motor can also be related to the torque (as in theory power is torque times impeller blade rotational speed), and thus, we expect that we may also be able to scale the power consumption by the diameter of particles.

In Fig. 13, we normalize the time-averaged torque and the average adjusted power values in Fig. 12 by the particle diameter for the three different cases of 1-mm, 2-mm, and 5-mm glass beads. It can be observed from Fig. 13a that the 1-mm particles have the highest normalized torque$\langle T\rangle/d$. It is interesting to note that, although the actual time-averaged torque increases with an increase in a particle diameter (see Fig. 12a), the normalized torque values$\langle T\rangle/d$, for the 2-mm and 5-mm particles are lower than that of the 1-mm particles. Moreover, the normalized torque $\langle T\rangle/d$ values for the 2-mm and 5-mm particles are fairly similar, implying that the torque exerted by the impeller on the granular material flowing in our bladed mixer complies with this theoretical scaling.

Discrepancy of the normalized torque values $\langle T \rangle / d$, for the 1-mm particles from the other cases might be due to the relatively wide particle size distribution of the 1-mm glass beads (see Section 2.2) and electrostatic charges that could extensively affect flow behaviors of the 1-mm beads.

Similar trends are observed in Fig. 13b for the average adjusted power normalized by the particle diameter, (P*/d), as a function of the shear rate. As mentioned above, the power consumption of the motor can in theory be related to the torque since power is torque times impeller blade rotational speed. We have examined if there is a simple relationship between the torque and the adjusted power, and we have not observed a direct relationship between the average torque values and the adjusted power. Once again, we hypothesize that this is because we have assumed that the power needed to run the motor when the mixer is not under load (empty mixer) equals the power needed to run the motor when the motor is under load (charged mixer). As we discussed previously, this assumption may not be true for all conditions and may contribute to the adjusted power results not being simply related to the torque. Further work is needed to understand this relationship.

3.6 Effect of Material Fill Height and Scale-up

Barczi et al. studied the effect of the granular bed depth on particle flow and homogenization in a vertical bladed mixer with two flat blades using the DEM technique. They observed that both macroscopic and microscopic flow patterns were affected by the

packed-bed depth and the blade rotational rate. Remy et al. carried out DEM simulations of bladed mixers at different scales and found that the total weight of the particle bed in a bladed mixer was an important parameter affecting stress profiles and granular flow behaviors. In this part, we will examine the effect of the amount of granular material, reported as the fill height in the mixer, on measured torque and power. To do so, 5-mm glass beads and a lead weight were used in the experiments in this section to imitate the hydrostatic pressure experienced by the impeller blades. A circular lead weight was placed on a circular-cut piece of cardboard which was inserted through the impeller shaft assembly. The lead weight and the cardboard sat on top of the glass beads and distributed the normal load onto the particle bed during agitation to mimic the hydrostatic pressure experienced in the mixer. The experiments were carried out for the following different initial fill heights of beads: 30 mm (H/D = 0.30), 60 mm (H/D = 0.60), and 85 mm (H/D = 0.85). It was determined that mass of the lead weight (530 g) was equivalent to the mass of a particle bed fill height of 44 mm. This information was used to increase the fill height without actually using glass beads. For the 85-mm fill height, we performed two different sets of experiments.

One scenario was using the beads actually filled up to 85 mm (H/D = 0.85), and the other setting was using the glass beads filled up to 41 mm plus the lead weight (equivalent to mm) on top (which we referred to as ‘‘Effective H/D = 0.85”). For the ‘‘Effective H/D = 1.04”, we placed the lead weight on top of the 60-mm fill height of the beads. It should be noted that the particle size of the beads used in these experiments was 5 mm. This

was different from the other cases because the 2-mm particles were smaller than the hole through which the lead weight was inserted onto the impeller shaft. Because of this, the 2-mm beads would escape upward through this hole and get on top of the lead weight, making the lead weight sink into the particle bed. Therefore, in order to overcome this problem, glass beads with a 5-mm particle size were used instead in the experiments in this section.

All experiments in this part were performed using the standard impeller blades (Fig. 3a). Additionally, all other process parameters were the same as those in the base case. Fig. 14 shows the time-averaged torque and the average adjusted power results for cases with different fill heights of the glass beads as a function of the dimensionless shear rate. It can be observed from Fig. 14a that the shallow bed (H/D = 0.30) of 5-mm beads exerts the lowest normal load on the impeller blades, and thus the lowest values of torque are measured. As the amount of material in the bladed mixer increases, the experimentally measured torque generally increases with the fill height of the beads.

The glass beads filled up to the 85-mm fill height (H/D = 0.85) yields comparable results to the case where the lead weight was placed on top of the material (Effective H/D = 0.85), implying that the lead weight can be a good representative of the normal load applied on the granular bed. In general, for the 104-mm fill height (Effective H/D = 1.04), the largest torque values are measured due to the largest amount of hydrostatic pressure experienced by the impeller blades during agitation. Similar trends for the average

adjusted power in the shallow bed granular system (H/D = 0.30) plotted as a function of the dimensionless shear rate can be seen in Fig. 14b. A scale-up relationship for deep granular beds varying the material fill height in a bladed mixer can be then developed from the average torque and adjusted power information. From Eq. (2), it can be rearranged to the following expression:

$$\vec{\mathrm{T}} = 2\pi R_{cyl}^2 \mathrm{H}\langle\tau_{\theta r}\rangle \qquad (9)$$

Note that the impeller torque ($\vec{\mathrm{T}}$) is proportional to the average shear stress $\tau_{\theta r}$ multiplied by the height (H) of the particle bed when the blades are rotating. In addition, Remy et al. [5] found that, for non-cohesive materials, Coulomb's law of friction was observed and the shear stress was proportional to the normal stress. The normal stress is in turn determined by the mass of powder in the mixer. In previous work, it has been observed that the mass of powder in the mixer was a critical parameter in terms of the powder flow patterns during the high shear mixing process [34]. In a bladed mixer, it was observed that the average shear stress $\tau_{\theta r}$ could be related to the hydrostatic pressure acting on the material [5]:

$$\langle\tau_{\theta r}\rangle = \mu\rho_{\mathrm{bulk}} g H \qquad (10)$$

where μ is the bulk friction coefficient, ρ_{bulk} is the bulk density of the granular bed, g is the acceleration due to gravity, and H is the fill height of the bed. It will be assumed that

changes in the granular bed bulk density ρ_{bulk} during agitation are negligible, i.e., ρ_{bulk} is approximately constant within the flow regimes we are investigating. This implies that the height, H of the granular bed does not change with rotation rate. We indeed observed in our experiments that when the blades are rotating the total height of the granular bed is approximately the same as the granular bed initial height at a stationary state. Substituting Eq. (10) into Eq. (9), the following relationship is derived subsequently:

$$\vec{\mathrm{T}} = 2\pi\mu\rho_{\mathrm{bulk}} g R^2_{\mathrm{cyl}} H^2 \qquad (11)$$

Expression (11) implies that the measured impeller torque scales by the square of the material fill height $\vec{\mathrm{T}}\alpha\ H^2$ in a bladed mixer when all other parameters are constant.

In Fig. 15, we normalize the experimentally measured time averaged torque $\vec{\mathrm{T}}$ and the average adjusted power P* values in Fig. 14 by the square of the granular bed fill height (H^2) for each case. The normalized torque $\langle T\rangle/H^2$ results shown in Fig. 15a illustrate that all of the normalized torque data points for the deep particle beds (H/D ≥ 0.60) essentially collapse into one single curve. It is interesting to note that, even though the actual time-averaged torque increases with an increase in the material fill height (see Fig. 14a), the normalized torque $\langle T\rangle/H^2$ for all deep granular bed cases (H/D ≥ 0.60) is lower than that of the shallow bed case (H/D = 0.30). Moreover, the fact that the normalized torque $\langle T\rangle/H^2$ values for the deep particle beds (H/D ≥ 0.60) collapse into one single curve, with the exclusion of the shallow bed case (H/D = 0.30), implies that the impeller torque exerted on deep granular beds behaves differently from that in a shallow bed. We

hypothesize this difference in the shallow bed case is because particles on the surface of the shallow bed can form heaps and valleys freely when the impeller blades are rotating, resulting in significant changes in the bed height and the bulk density especially at high shear rates which can in turn affect the torque scaling relationship in Eq. (11). An analogous principle can be applied to the impeller blade power consumption, and the normalized adjusted power P^*/H^2 results are depicted in Fig. 15b. Similar trends are observed for the normalized adjusted power P^*/H^2 both in the shallow and deep particle bed cases for the entire range of the granular flow regime.

3.7 Figures for Chapter 3

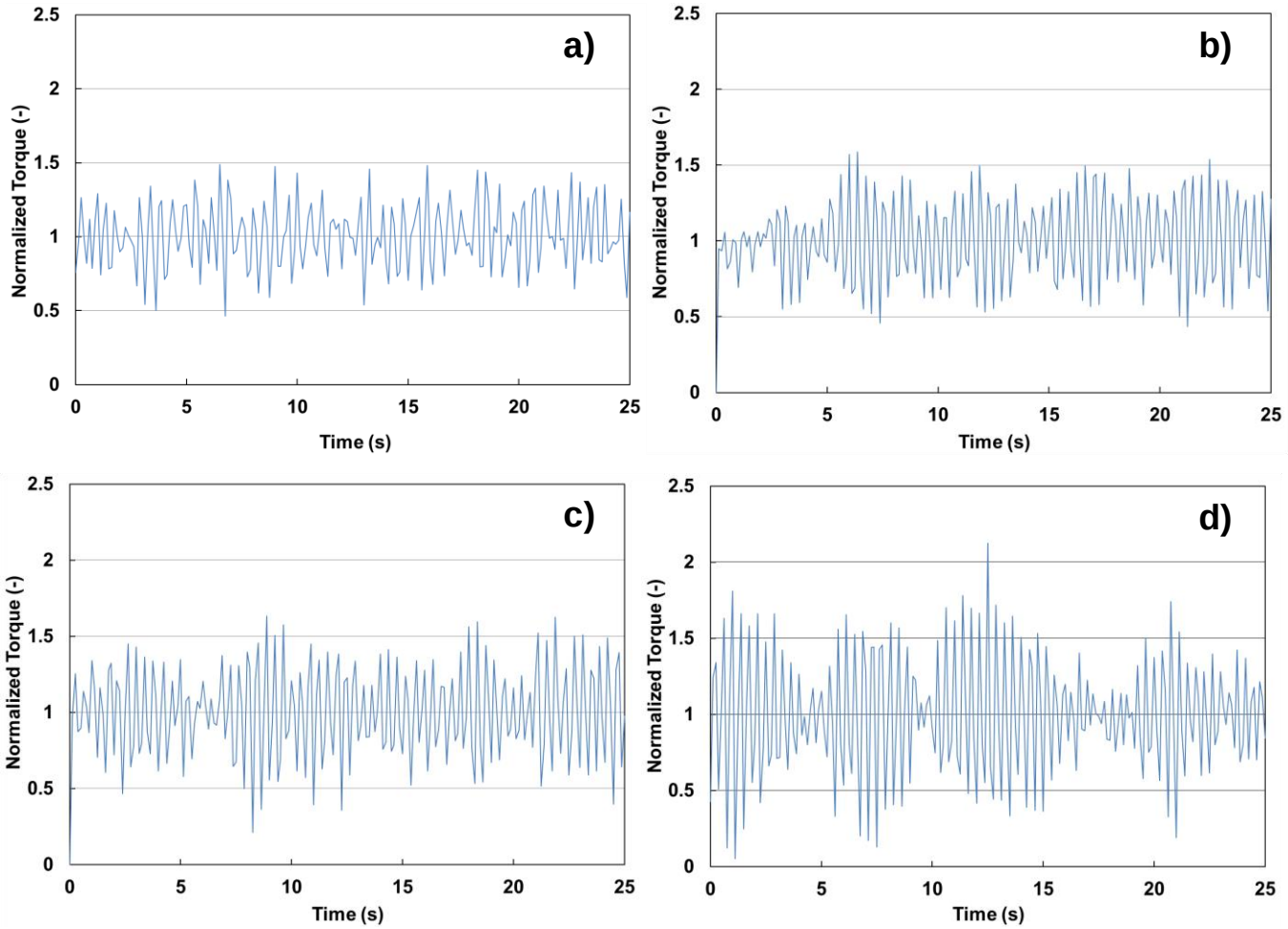

Fig. 4. Normalized torque ($\vec{T}^*$) fluctuation profiles at steady state for different blade rotational speeds: (a) 10 RPM, (b) 20 RPM, (c) 60 RPM, and (d) 200 RPM. The normalized torque values shown in this figure are the instantaneous torques divided by the time-averaged torque at each shear rate. Torque signal measurements were recorded every 0.125 s.

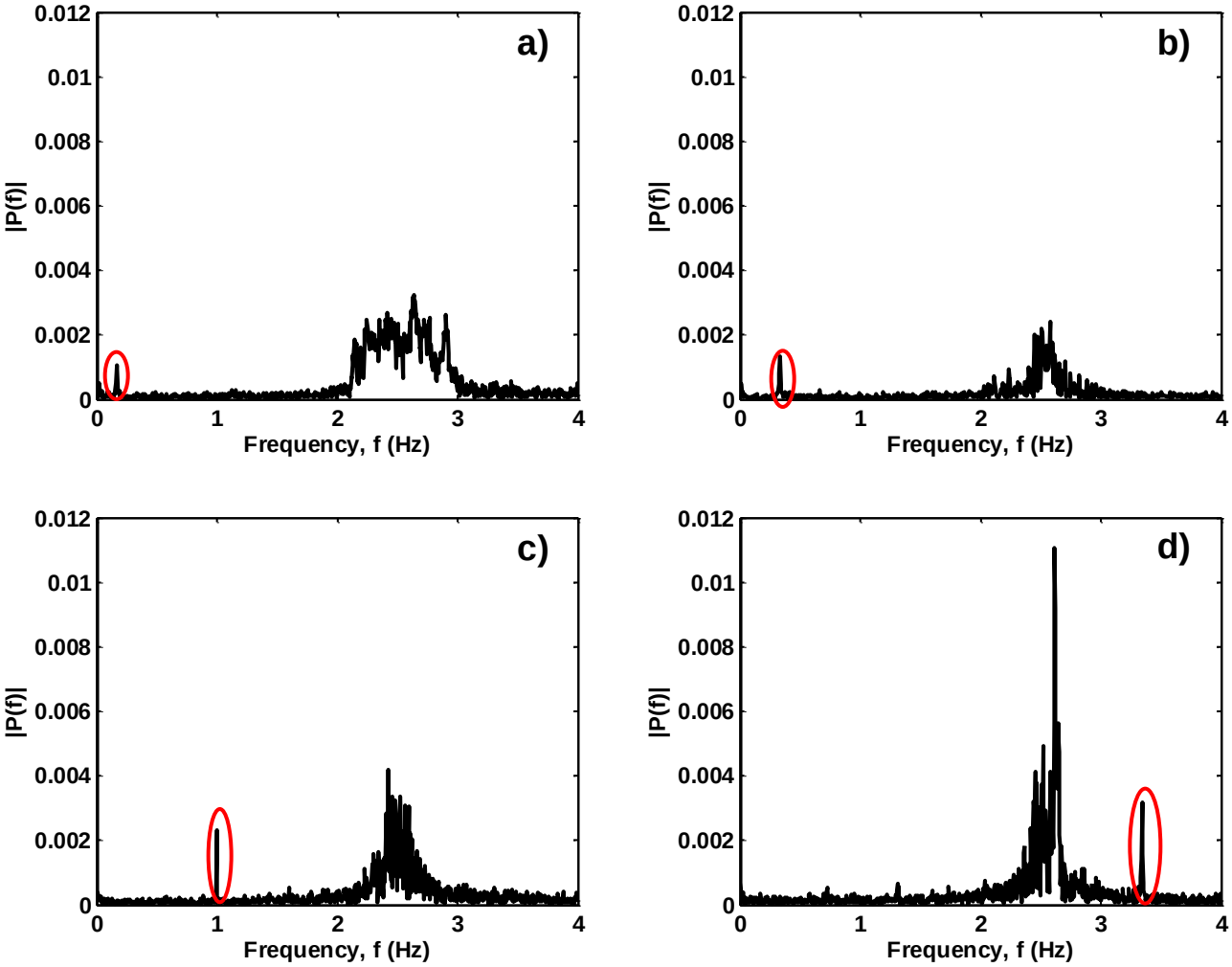

Fig. 5. Single-sided amplitude spectrums of the fast Fourier transform (FFT) torque signals for different blade rotational speeds: (a) 10 RPM, (b) 20 RPM, (c) 60 RPM, and (d) 200 RPM. Torque signal measurements were recorded every 0.125 s.

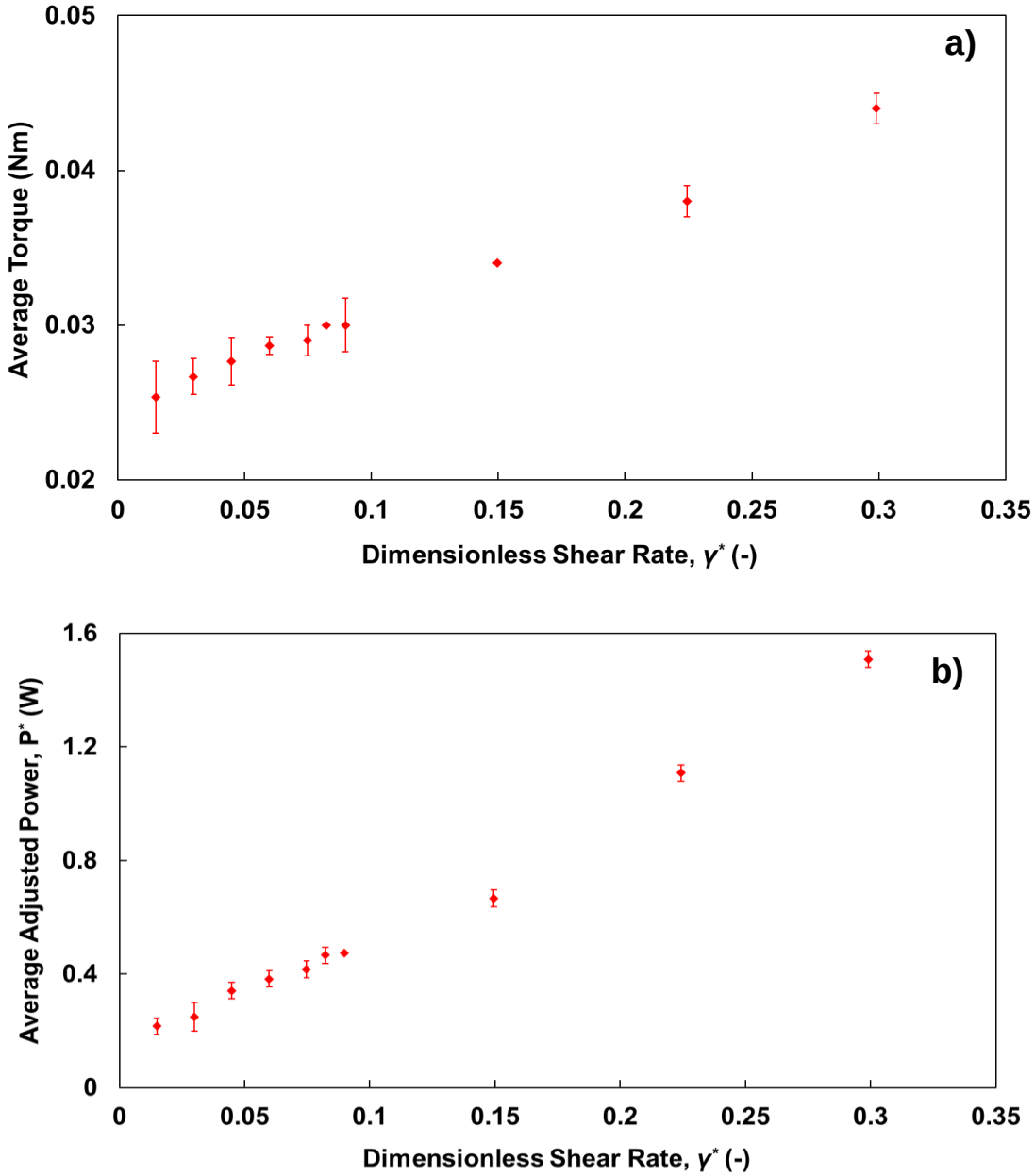

Fig. 6. Granular flow properties as a function of the dimensionless shear rate (γ^*) for "the standard case": (a) the time-averaged impeller torque and (b) the average adjusted power (P^*). The experiments were performed using red glass beads of 2-mm diameter loaded to a 30-mm fill height (shallow bed, H/D = 0.30) and the standard impeller blades (4 blades with a 135° angle and 45 mm length). The adjusted power (P^*) was obtained by subtracting the power draw at a specific RPM for the empty mixer from the power draw for the impeller in the mixer loaded with particles.

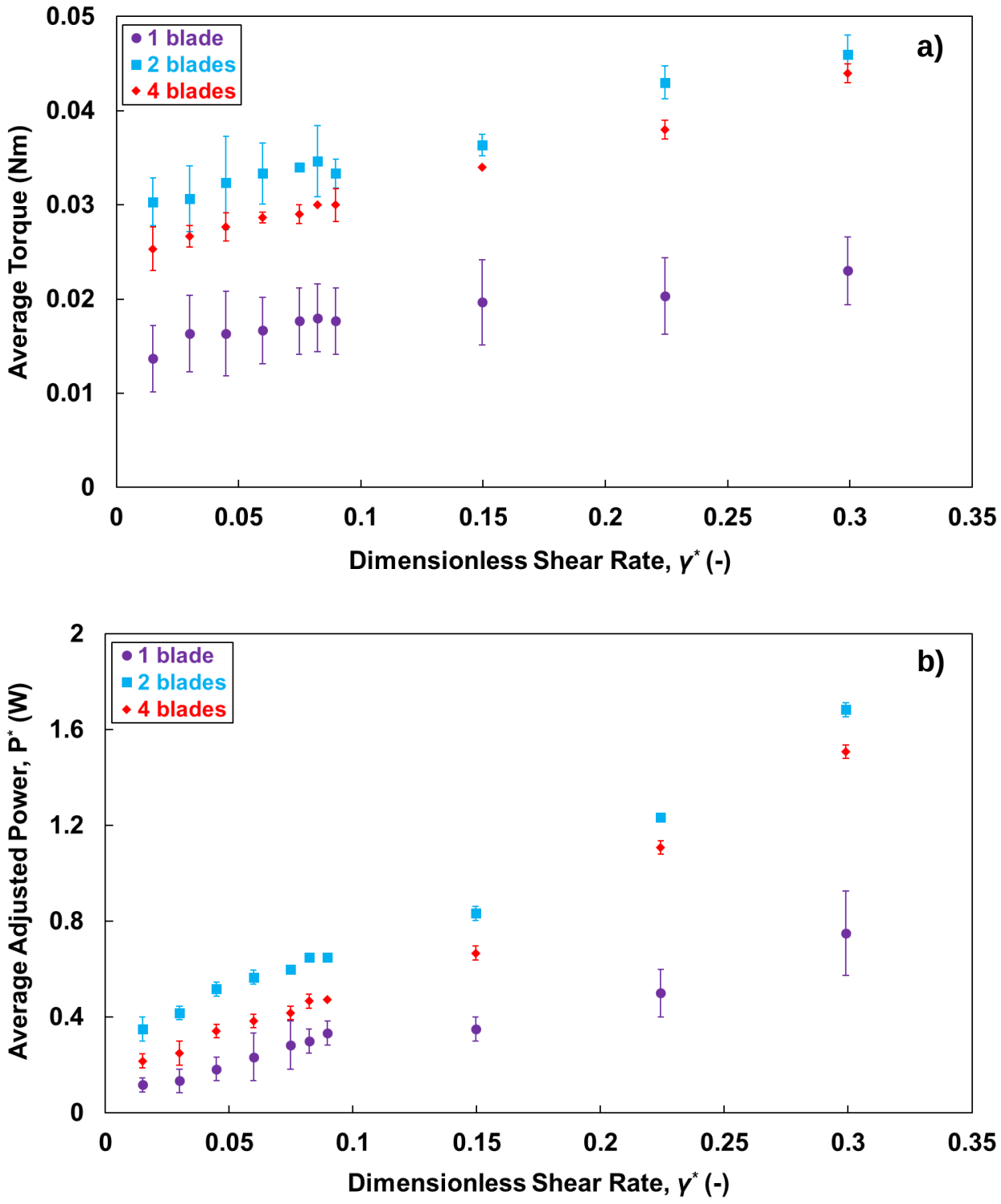

Fig. 7. Effect of the number of impeller blades on: (a) the average torque and (b) the average adjusted power as a function of the dimensionless shear rate. Impeller blades used in these sets of experiments have 135° angle and 45 mm length.

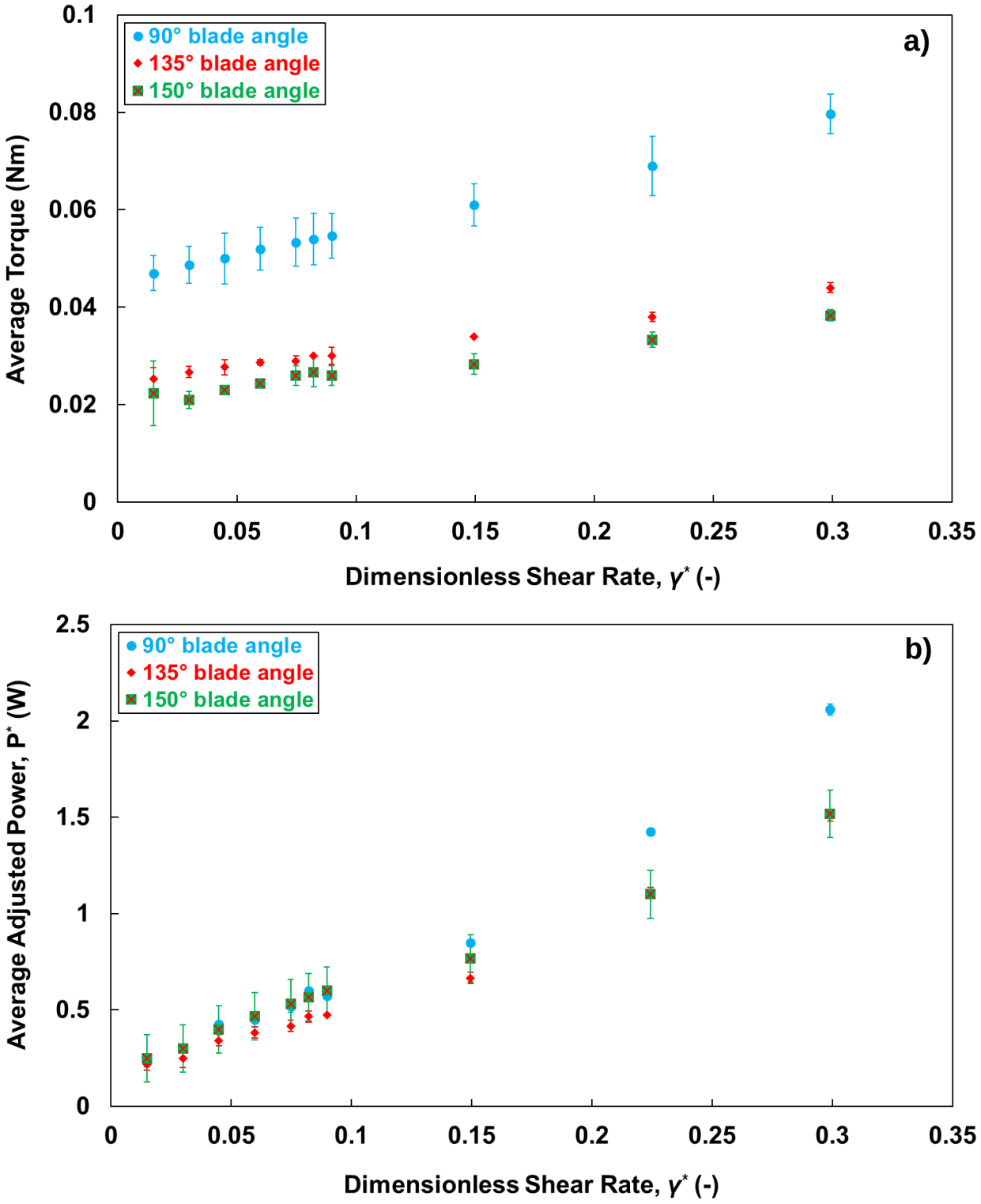

Fig. 8. Effect of the impeller blade angle on: (a) the average torque and (b) the average adjusted power as a function of the dimensionless shear rate. Impeller blades used in these sets of experiments have 4 blades and 45 mm length.

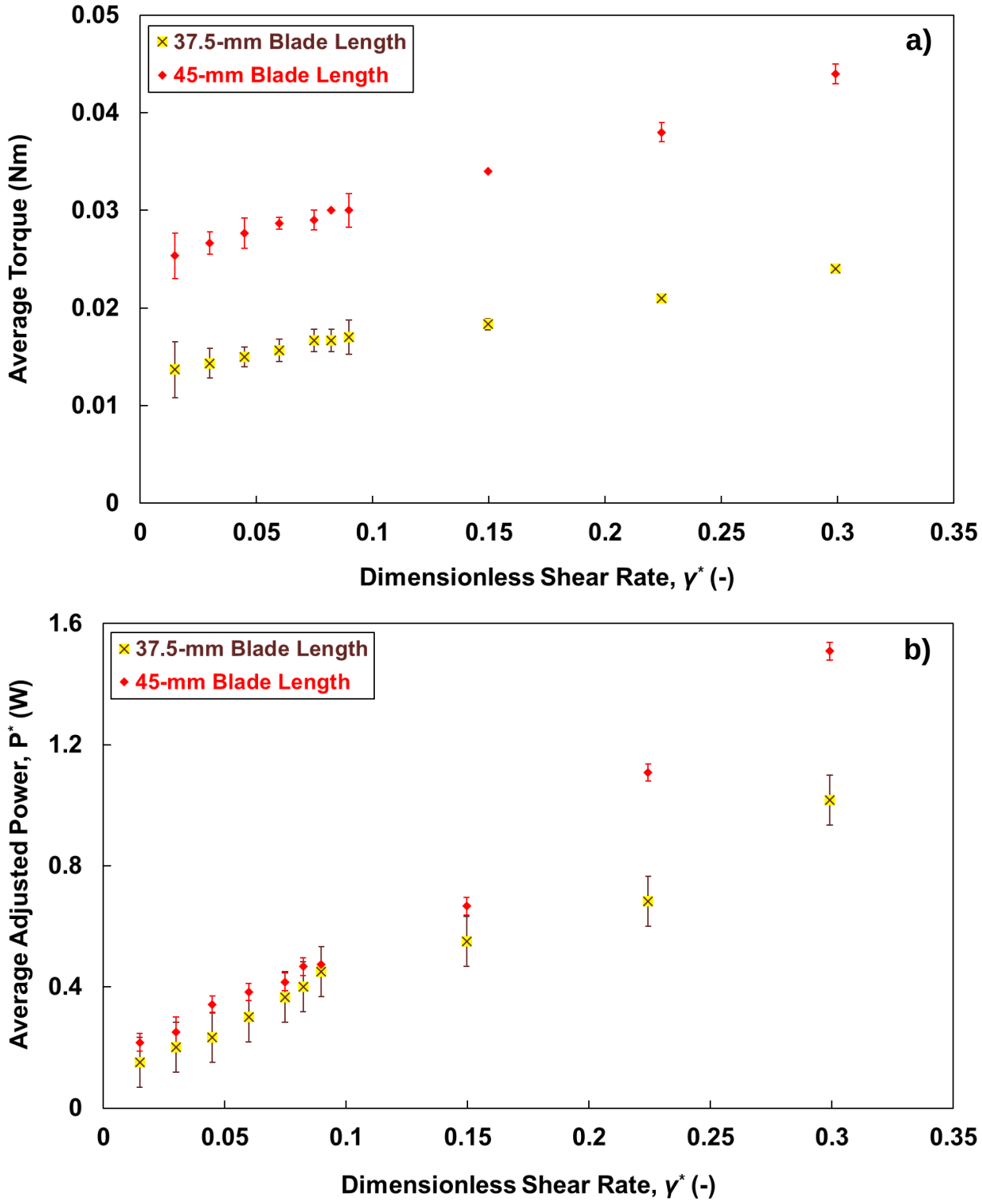

Fig. 9. Effect of the impeller blade length on: (a) the average torque and (b) the average adjusted power as a function of the dimensionless shear rate. Impeller blades used in these sets of experiments for both cases have 4 blades and 135° angle.

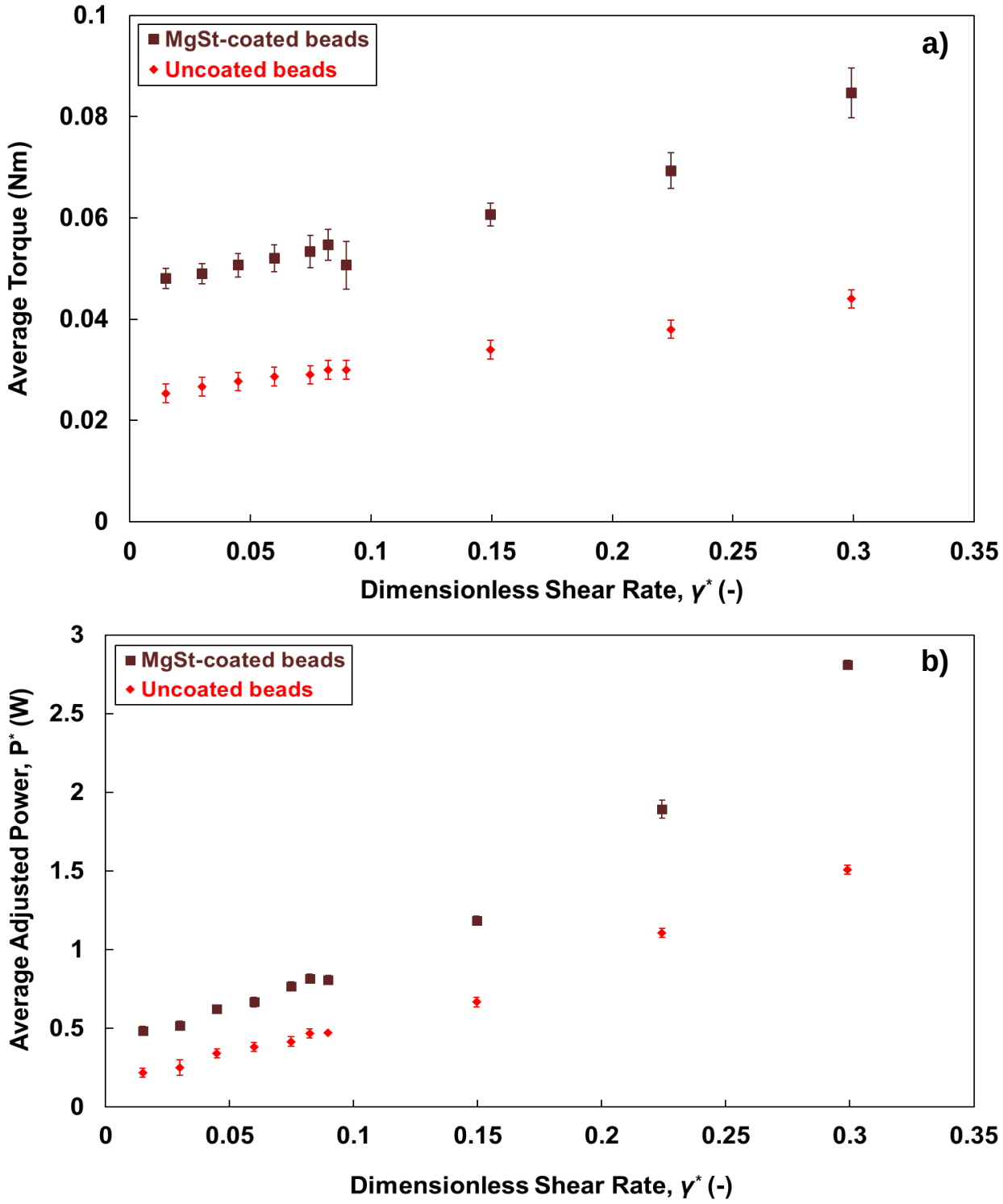

Fig. 10. Effect of the macroscopic friction coefficient (μ) of particles on: (a) the average torque and (b) the average adjusted power as a function of the dimensionless shear rate. Experiments were performed using the standard impeller blades and the glass beads with a diameter of 2 mm loaded to a 30-mm fill height (H/D = 0.30).

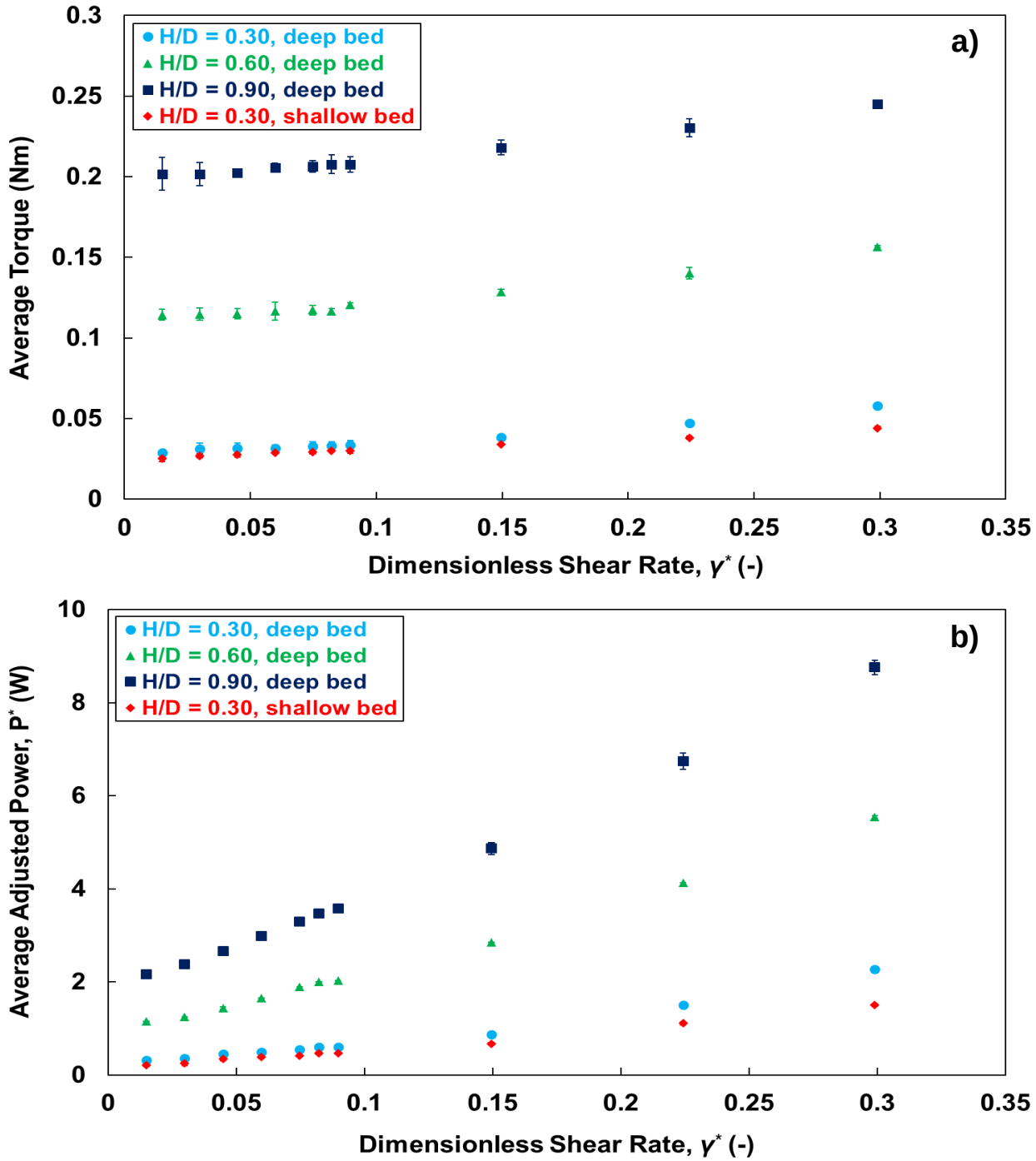

Fig. 11. Effect of the impeller blade position in a deep granular bed (90-mm fill height) on: (a) the time-averaged torque and (b) the average adjusted power as a function of the dimensionless shear rate, compared to those values in a shallow bed (30-mm fill height just covering the top tip of the blades). Blade position in a deep bed: top (H/D = 0.30), middle (H/D = 0.60), and bottom (H/D = 0.90). Experiments were performed using the standard impeller blades and the glass beads with a diameter of 2 mm.

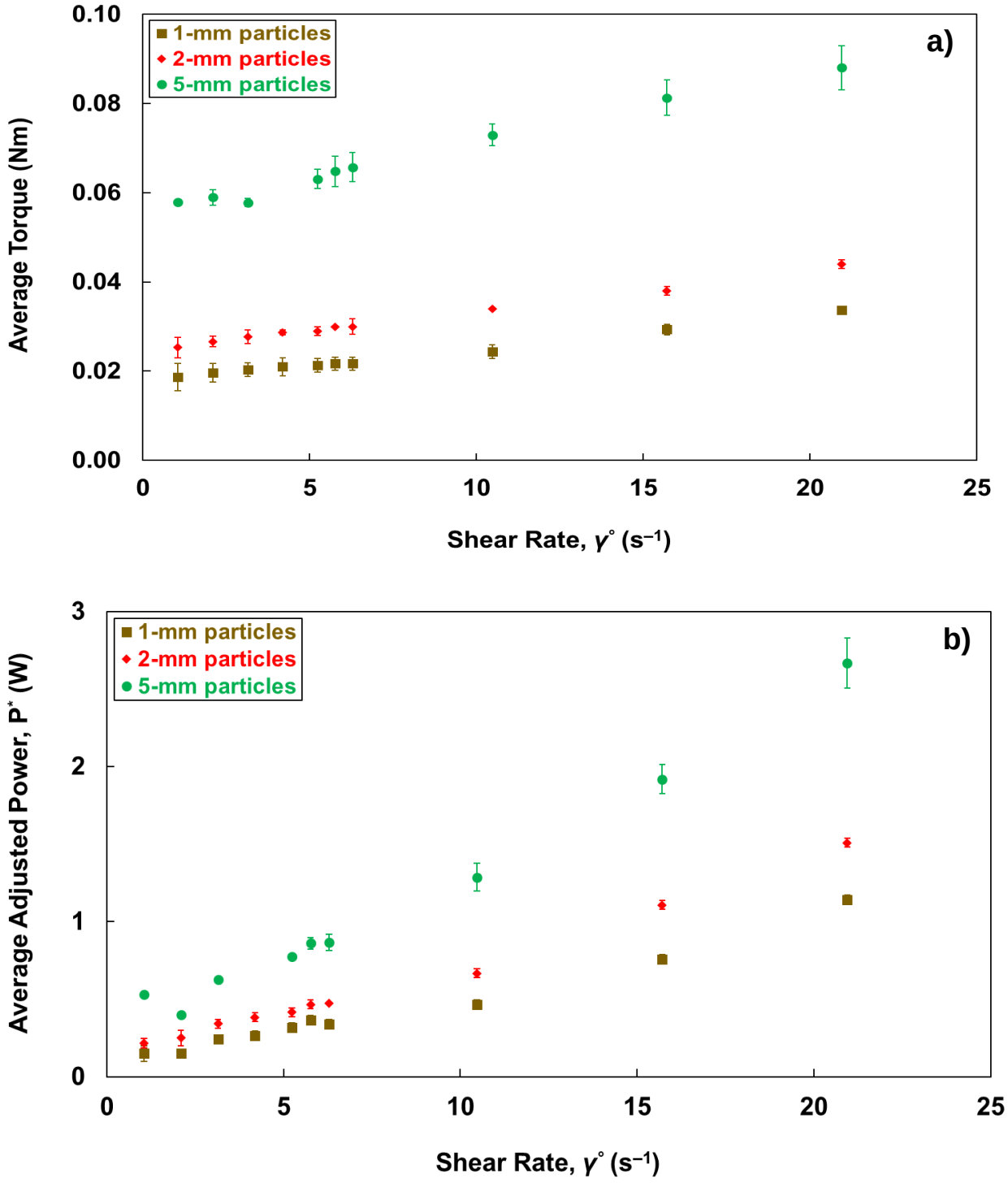

Fig. 12. Effect of the particle size on: (a) the average torque and (b) the average adjusted power drawn from experiments as a function of the shear rate $\dot{\gamma}$. Experiments were performed using the standard impeller blades, and the granular bed was filled up to a 30-mm height (H/D = 0.30) for all particle sizes.

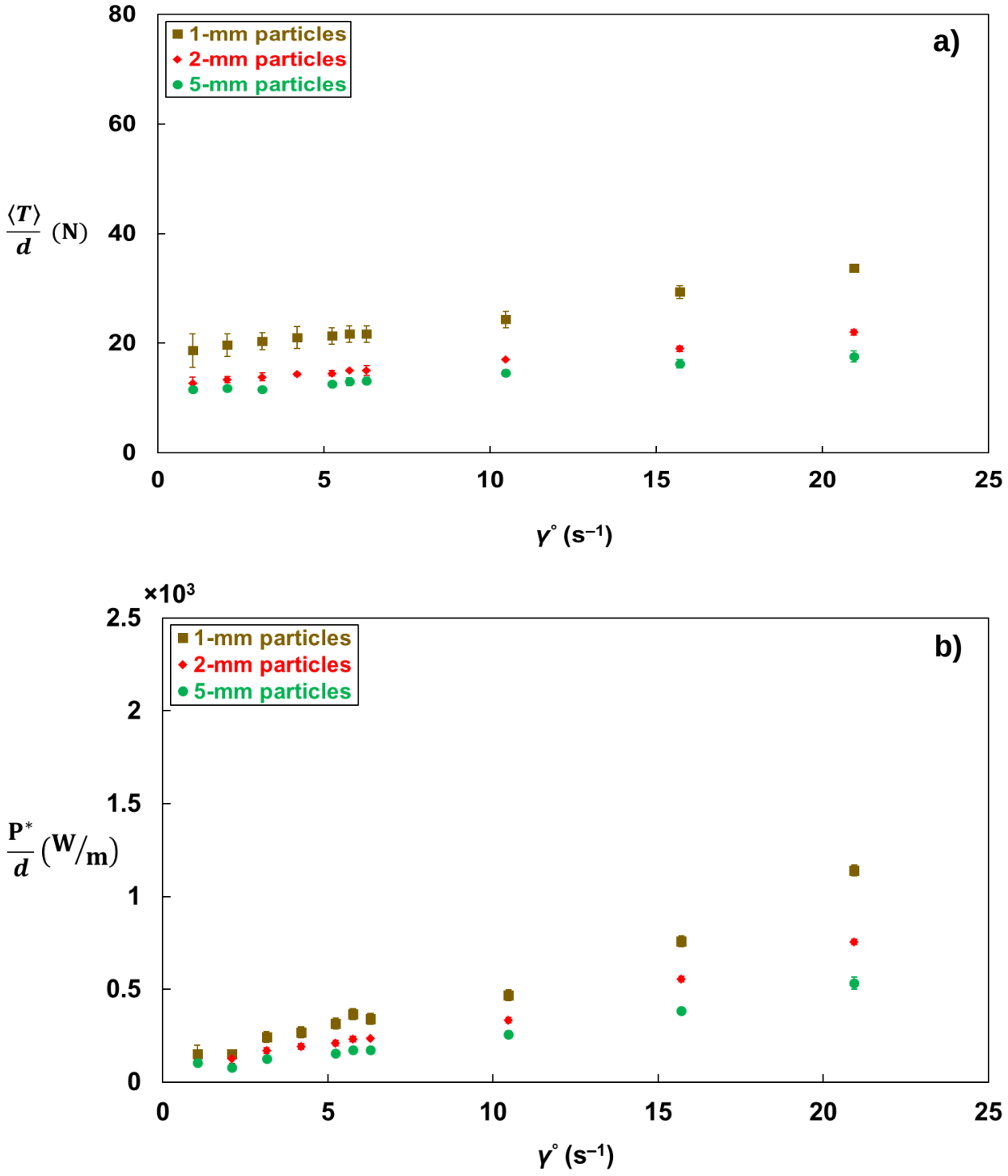

Fig. 13. (a) The time-averaged normalized torque, $\langle T \rangle / d$, and (b) the average normalized adjusted power, P^*/d, plotted as a function of the shear rate $\dot{\gamma}$. Experiments were performed using the standard impeller blades, and the granular bed was filled up to a 30-mm height (H/D = 0.30) for all particle sizes. Note that the y-axis in Fig. 13b is multiplied by a factor of 10^3.

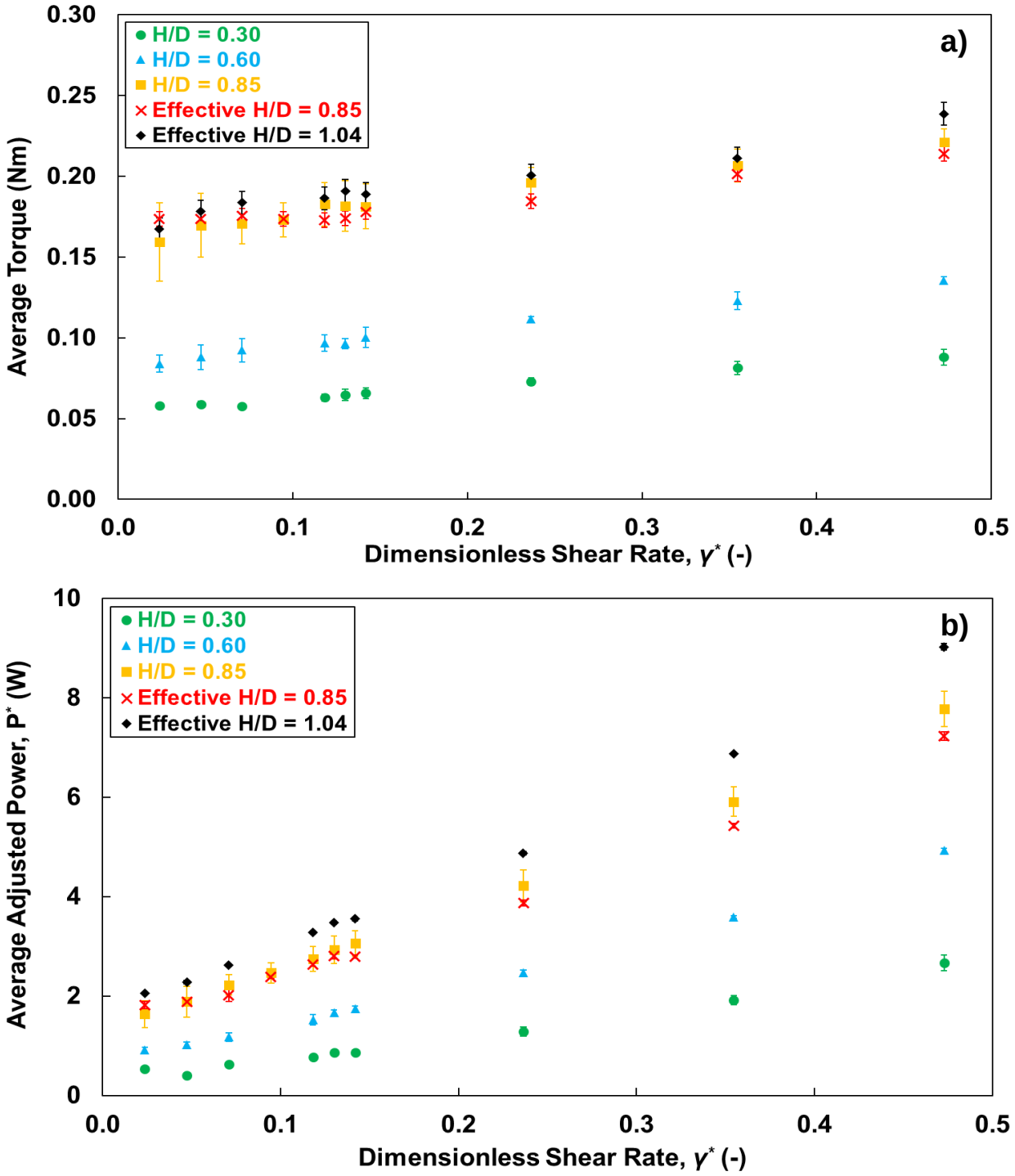

Fig. 14. Effect of the amount of materials in a bladed mixer, reported as the *H*/*D* ratio, on: (a) the time-averaged torque and (b) the average adjusted power as a function of the dimensionless shear rate. Experiments were performed using the standard impeller blades and the glass beads with a diameter of 5 mm. The effective *H*/*D* ratios indicate usage of a lead weight instead of using actual particle mass.

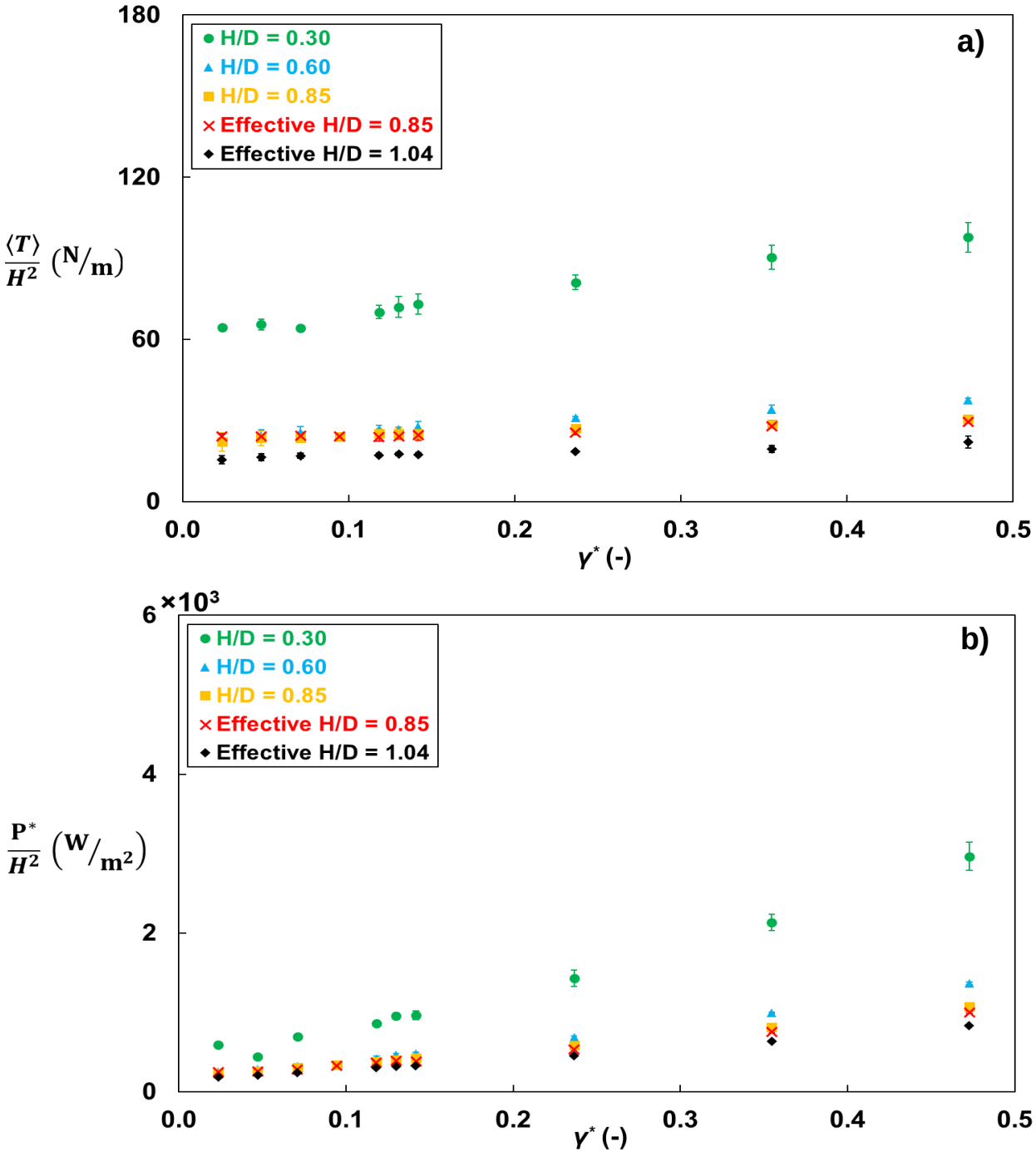

Fig. 15. (a) The time-averaged torque $\langle \vec{T} \rangle$ and (b) the average adjusted power P^* values in Fig. 14 were normalized by square of the height (H^2) of the granular material filled in a bladed mixer plotted as a function of the dimensionless shear rate. Experiments were performed using the standard impeller blades and the glass beads with a diameter of 5 mm. The effective *H*/*D* ratios indicate usage of a lead weight instead of using actual particle mass. Note that the y-axis in Fig. 15b is multiplied by a factor of 10^3.

4 CONCLUSION

Experiments were performed on monodisperse spherical glass beads flowing in a cylindrical bladed mixer agitated by an impeller. Experimental measurements of the torque exerted by the impeller blades on the granular bed were achieved by using a torque table and a data acquisition system. Power consumed by the motor to move an agitator through the particle bed was also experimentally measured using a power meter. The effects of various impeller blade design configurations and material properties on the agitation torque and power were examined as a function of the impeller blade rotational speed. For “the base case”, which was composed of 2-mm diameter glass beads filled up to a 30-mm height (H/D = 0.30) that just covered the span of the blades and considered as a shallow bed using “the standard impeller blades”, the time-averaged torque values at low shear rates were slightly increasing within the quasi-static regime of granular flow behaviors. This was then followed by a linear increase in the torque in the intermediate region as the shear rate increased. This trend for the impeller torque was similar to what was observed for the adjusted power consumption. Data analysis in “the base case” revealed that fluctuation of torque values was fairly constant in the quasi-static region and increased with an increasing blade rotational speed in the intermediate flow regime. FFT spectrums for “the base case” showed peaks at frequencies corresponding to the impeller blade rotational rates.

This research demonstrates that the torque values and the power readings measured from the mixing system were sensitive to several factors including the impeller blade configurations (number, angle, and length of blades), the particle size and friction coefficient, the blade position in a deep granular bed, and the fill height of the glass beads. The time-averaged torque was dependent on the number of impeller blades used in the mixer; the 2- and 4-bladed mixers exerted greater torque than the 1-bladed mixer on the particle bed due to the larger blade-particle tangential forces. The torque values also increased with an increase in the blade length and with a decrease in the blade pitch angle. Furthermore, at higher fill heights of the granular material, greater torque values and power readings could be measured. The highest torque and power measurements were recorded for the case where the impeller blades were placed at the most bottom position (H/D = 0.90) of the deep particle bed. This was because of the hydrostatic pressure from the material on top of the blades. Moreover, the average torque and adjusted power were a strong function of material properties including particle diameter and surface roughness. Larger particle sizes and a greater friction coefficient resulted in higher magnitudes of the torque and power. In addition, the time-averaged torque and power consumption for the 2- and 5-mm bead cases qualitatively scaled with particle diameter.

It was demonstrated that granular flow behaviors in a shallow bed were different from those in the deep bed. As the amount of material in the bladed mixer increased, the experimentally measured torque also increased. In the deep particle bed, the measured

torque was independent of the shear rate in a quasi-static regime and then linearly increased as the blade rotational speed increased in the intermediate regime. Moreover, the clear distinction between these two regions could be observed in the deep granular bed, which could not be obviously differentiated in the shallow bed case. A scale-up relationship for deep granular beds varying the material fill height in a bladed mixer was then developed from the average torque and adjusted power information. The time averaged torque and average adjusted power consumption qualitatively scaled with square of the material fill height in a deep granular bed.

The results from research work in this chapter provide an insight on how the impeller blade configurations and material properties affect the agitation torque and power measured as a function of a process parameter in granular systems flowing in a bladed mixer. These findings complement our preceding knowledge and provide better understanding with regard to processing of solid particulate systems. At the same time these results are for a limited number of parameters, and future work is needed to validate that the results of this study hold for other parameter values. Further research should be conducted to study the effect of other material properties (e.g. cohesive particles), equipment configurations (e.g. different types of mixers), and other process parameters on particulate flow and mixing in a bladed mixer. Experiments can be done by adding and varying the amount of water in a granular bed to investigate the effect of cohesion on measured torque and power consumed by the impeller blades. In addition, results of the parametric sensitivity analysis for the impeller blade torque and power

consumption found in this research can be extended further by performing experiments in larger scale mixers. DEM simulations in a similar geometry can also be carried out by varying the aforementioned factors to provide information about torque and power.

5 REFERENCES

[1] F.J. Muzzio, A. Alexander, C. Goodridge, E. Shen, T. Shinbrot, Solids mixing part a: fundamentals of solids mixing, in: E.L. Paul, V.A. Atiemo-Obeng, S.M. Kresta (Eds.), Handbook of Industrial Mixing: Science and Practice, John Wiley & Sons Inc, 2004, pp. 887–985.

[2] J. Havlica, K. Jirounkova, T. Travnickova, M. Kohout, The effect of rotational speed on granular flow in a vertical bladed mixer, Powder Technol. 280 (2015) 180–190.

[3] S. Radl, E. Kalvoda, B.J. Glasser, J.G. Khinast, Mixing characteristics of wet granular matter in a bladed mixer, Powder Technol. 200 (2010) 171–189.

[4] S. Oka, O. Kašpar, V. Tokárová, K. Sowrirajan, H. Wu, M. Khan, F. Muzzio, F. Šteˇpánek, R. Ramachandran, A quantitative study of the effect of process parameters on key granule characteristics in a high shear wet granulation process involving a two component pharmaceutical blend, Adv. Powder Technol. 26 (2015) 315–322.

[5] B. Remy, W. Kightlinger, E.M. Saurer, N. Domagalski, B.J. Glasser, Scale-up of agitated drying: effect of shear stress and hydrostatic pressure on active pharmaceutical ingredient powder properties, AIChE J. 61 (2015) 407–418.

[6] E.W. Conder, A.S. Cosbie, J. Gaertner, W. Hicks, S. Huggins, C.S. MacLeod, B. Remy, B.-S. Yang, J.D. Engstrom, D.J. Lamberto, C.D. Papageorgiou, The pharmaceutical drying unit operation: an industry perspective on advancing the science and development approach for scale-up and technology transfer, Org. Process Res. Dev. 21 (2017) 420–429.

[7] M. Ebrahimi, E. Siegmann, D. Prieling, B.J. Glasser, J.G. Khinast, An investigation of the hydrodynamic similarity of single-spout fluidized beds using CFD-DEM simulations, Adv. Powder Technol. 28 (2017) 2465–2481.

[8] A. Chaudhury, A. Niziolek, R. Ramachandran, Multi-dimensional mechanistic modeling of fluid bed granulation processes: an integrated approach, Adv. Powder Technol. 24 (2013) 113–131.

[9] Y. Sato, H. Nakamura, S. Watano, Numerical analysis of agitation torque and particle motion in a high shear mixer, Powder Technol. 186 (2008) 130–136.

[10] Y. Wang, T. Li, F.J. Muzzio, B.J. Glasser, Predicting feeder performance based on material flow properties, Powder Technol. 308 (2017) 135–148.

[11] B. Remy, J.G. Khinast, B.J. Glasser, Wet granular flows in a bladed mixer: experiments and simulations of monodisperse spheres, AIChE J. 58 (2012) 3354–3369.

[12] A. Lekhal, S.L. Conway, B.J. Glasser, J.G. Khinast, Characterization of granular flow of wet solids in a bladed mixer, AIChE J. 52 (2006) 2757–2766.

[13] S. Radl, D. Brandl, H. Heimburg, B.J. Glasser, J.G. Khinast, Flow and mixing of granular material over a single blade, Powder Technol. 226 (2012) 199– 212.

[14] D.F. Bagster, J. Bridgwater, The measurement of the force needed to move blades through a bed of cohesionless granules, Powder Technol. 1 (1967) 189– 198.

[15] R. Chandratilleke, A. Yu, J. Bridgwater, K. Shinohara, Flow and mixing of cohesive particles in a vertical bladed mixer, Ind. Eng. Chem. Res. 53 (2014) 4119–4130.

[16] G.R. Chandratilleke, A.B. Yu, J. Bridgwater, A DEM study of the mixing of particles induced by a flat blade, Chem. Eng. Sci. 79 (2012) 54–74.

[17] G.R. Chandratilleke, A.B. Yu, J. Bridgwater, K. Shinohara, A particle-scale index in the quantification of mixing of particles, AIChE J. 58 (2012) 1099–1118.

[18] P.C. Knight, J.P.K. Seville, A.B. Wellm, T. Instone, Prediction of impeller torque in high shear powder mixers, Chem. Eng. Sci. 56 (2001) 57– 71.

[19] S. Wu, S.S. Panikar, R. Singh, J. Zhang, B. Glasser, R. Ramachandran, A systematic framework to monitor mulling processes using Near Infrared spectroscopy, Adv. Powder Technol. 27 (2016) 1115–1127.

[20] A. Chaudhury, A. Kapadia, A.V. Prakash, D. Barrasso, R. Ramachandran, An extended cell-average technique for a multi-dimensional population balance of granulation describing aggregation and breakage, Adv. Powder Technol. 24
(2013) 962–971.

[21] T. Kumaresan, J.B. Joshi, Effect of impeller design on the flow pattern and mixing in stirred tanks, Chem. Eng. J. 115 (2006) 173–193.

[22] M. Ritala, P. Holm, T. Schaefer, H.G. Kristensen, Influence of liquid bonding strength on power consumption during granulation in a high shear mixer, Drug Dev. Ind. Pharm. 14 (1988) 1041–1060.

[23] T. Jirout, F. Rieger, Impeller design for mixing of suspensions, Chem. Eng. Res. Des. 89 (2011) 11 –1151.

[24] M. Ierapetritou, F. Muzzio, G. Reklaitis, Perspectives on the continuous manufacturing of powder-based pharmaceutical processes, AIChE J. 62 (2016) 1846–1862.

[25] S.L. Lee, T.F. O'Connor, X. Yang, C.N. Cruz, S. Chatterjee, R.D. Madurawe, C.M.V. Moore, L.X. Yu, J. Woodcock, Modernizing pharmaceutical manufacturing: from batch to continuous production, J. Pharm. Innov. 10 (2015) 191–199.

[26] M. Sen, R. Ramachandran, A multi-dimensional population balance model approach to continuous powder mixing processes, Adv. Powder Technol. 24 (2013) 51–59.

[27] A.U. Vanarase, F.J. Muzzio, Effect of operating conditions and design parameters in a continuous powder mixer, Powder Technol. 208 (2011) 26–36.

[28] A.U. Vanarase, J.G. Osorio, F.J. Muzzio, Effects of powder flow properties and shear environment on the performance of continuous mixing of pharmaceutical powders, Powder Technol. 246 (2013) 63–72.

[29] C.S. Campbell, Granular shear flows at the elastic limit, J. Fluid Mech. 465 (2002) 261–291.

[30] C.S. Campbell, Self-diffusion in granular shear flows, J. Fluid Mech. 348 (1997) 85–101.

[31] C.S. Campbell, C.E. Brennen, Computer simulation of granular shear flows, J. Fluid Mech. 151 (1985) 167–188.

[32] T. Weinhart, R. Hartkamp, A.R. Thornton, S. Luding, Coarse-grained local and objective continuum description of three-dimensional granular flows down an inclined surface, Phys. Fluids 25 (2013) 070605.

[33] T. Weinhart, C. Labra, S. Luding, J.Y. Ooi, Influence of coarse-graining parameters on the analysis of DEM simulations of silo flow, Powder Technol.
293 (2016) 138–148.

[34] M. Cavinato, R. Artoni, M. Bresciani, P. Canu, A.C. Santomaso, Scale-up effects on flow patterns in the high shear mixing of cohesive powders, Chem. Eng. Sci.
102 (2013) 1–9.

[35] T. Shinbrot, K. LaMarche, B.J. Glasser, Triboelectrification and razorbacks: geophysical patterns produced in dry grains, Phys. Rev. Lett. 96 (2006), 178002
178001-178004.

[36] G.I. Tardos, S. McNamara, I. Talu, Slow and intermediate flow of a frictional bulk powder in the Couette geometry, Powder Technol. 131 (2003) 23–39.

[37] R.B. Bird, W.E. Stewart, E.N. Lightfoot, Transport Phenomena, Revised second ed., John Wiley & Sons Inc, New York, USA, 2007.

[38] A. Darelius, E. Lennartsson, A. Rasmuson, I. Niklasson Björn, S. Folestad, Measurement of the velocity field and frictional properties of wet masses in a high shear mixer, Chem. Eng. Sci. 62 (2007) 2366–2374.

[39] B. Remy, T.M. Canty, J.G. Khinast, B.J. Glasser, Experiments and simulations of cohesionless particles with varying roughness in a bladed mixer, Chem. Eng. Sci. 65 (2010) 57– 71.

[40] V. Boonkanokwong, B. Remy, J.G. Khinast, B.J. Glasser, The effect of the number of impeller blades on granular flow in a bladed mixer, Powder Technol. 302 (2016) 333–349.

[41] B. Remy, J.G. Khinast, B.J. Glasser, Discrete element simulation of free flowing grains in a four-bladed mixer, AIChE J. 55 (2009) 2035–2048.

[42] B. Remy, Granular flow, segregation and agglomeration in bladed mixers, in: Chemical and Biochemical Engineering, Chemical and Biochemical Engineering, Rutgers, The State University of New Jersey, New Brunswick, NJ, 2010, p. 285.